ORIGINAL ARTICLE

Delineation of flood risk terrains and rainfall visualisation in the North Western part of Ghana

Benjamin Wullobayi Dekongmen[1,2] · Amos Tiereyangn Kabo-bah[1] · Geophrey Kwame Anornu[3] · Komlavi Akpoti[4] · Mark Amo-Boateng[5] · Eric Ofosu Antwi[1,6] · Edward Oppong Boamah[7] · Emmanuel Daanoba Sunkari[8,9]

Abstract

Flooding, exacerbated by the challenges of climate change, poses a growing threat to communities in the Upper West Region (UWR) of Ghana. This persistent issue, particularly during the rainy seasons has subjected the region to several losses of properties and lives over the years. This has spurred the need for a comprehensive delineation of flood risk terrains (FRTs) and analysis of the rainfall patterns in the region. This study, therefore, started by analysing a digital elevation model (SRTM—DEM) using Jenks Natural Breaks Classification (JNBC) algorithm to delineate potential FRTs map within the region. Further, analysis was performed using Analytical Hierarchy Process Multi-Criteria Decision (AHP-MCD) with the incorporation of six spatial factors (Lineament Density, Elevation, Topographic Wetness Index, Drainage Density, Slope, and Aspect) to generate a comprehensive FRTs map. Climate Hazards Group InfraRed Precipitation with Station data (CHIRPS) from 1992 to 2022 were also visualized in a Jupyter Notebook to assess rainfall patterns in the UWR. Historical flood events data were also analysed to understand the trends of flood events impacts. From the findings, both the JNBC and AHP-MCD algorithms categorized the UWR's total area into five classes, namely; very high, high, moderate, low, and very low FRTs. The JNBC map had area coverages of 4% (856.278 km^2), 7% (1466.685 km^2), 12% (2418.642 km^2), 35% (7014.96 km^2), and 42% (8351.496 km^2) from very high risk to very low FRTs, respectively. Notably, the very high risk terrains and high risk terrains were predominantly located along the southeastern and eastern regions, particularly along the Kulpawn River and Sisili River in the UWR. The five classes AHP-MCD map also recorded areas as 0.004% (0.707 km^2), 21% (3830.02 km^2), 69% (12807.31 km^2), 10% (1827.011 km^2), and 0.062% (11.535 km^2) very high risk to very low FRTs, respectively. These findings further revealed a prevalence of high FRTs along stream and river networks. Interestingly, the validation of the AHP-MCD map over the ground truthing points indicated that the UWR is dominated by moderate FRTs (71.76%), underscoring the region's vulnerability to flooding. The visualization of the spatial rainfall distribution from 1992 to 2022, also highlighted the significance of heavy rainfall years, particularly in 2018, 2019, and 2021, and the month of August as consistent predictors of flood occurrences. A correlation matrix reinforces the strong connection between rainfall and flood-related impacts, such as affected populations, economic costs, and agricultural losses from 2016 to 2021. In light of these findings, UWR residents must prioritize flood-resilient crop cultivation and adhere to flood disaster safety protocols, especially during the critical month of August. These insights hold valuable implications for municipal, district, and community planning policies, offering a foundation for proactive sustainable flood risk mitigation and community resilience efforts in the region.

Keywords Flood · Analytical hierarchy process · Jenks natural breaks classification · Upper West Region · Rainfall · Spatial distribution

Introduction

Flood occurrences in the context of climate change have swept through several facets of the world (Armah et al. 2010; Aznar-crespo et al. 2021). Notably, the generation

---

of floods through riverine systems overflows, and overland flows under extreme rains has posed an ever increasing threat to natural resources and humanity (CRED 2018; Sofia and Nikolopoulos 2020). Significantly, the challenge becomes evident and rampant when the general land surfaces and drainage network systems are unable to discharge or convey excess rainwater after heavy downpours, as population

growth with rapid urban land uses changes (United Nations 2009; Le Polain De Waroux 2011; Sofia and Nikolopoulos 2020; Liu et al. 2023; Nearing et al. 2024; Rączkowska et al. 2024). In recent times, driving climate change and its increasing global warming have been ranked as the worst acceleration of environmental and hydrological extremities; floods and droughts (Garg et al. 2023; Bullen and Miles 2024; UNESCO 2023a, b; Nearing et al. 2024). Heavy rainfalls and land surface changes also play major roles in flood frequency and magnitude generation (Tarasova et al. 2023; Fischer and Schumann 2024). Though some studies have ascribed flood occurrences to hydro-meteorology (Tabari 2020; Alifu et al. 2022), perennial flood impacts, severity, and risks are also driven by three (3) core phenomena; vulnerability, hazards, and exposure (Hudson and Berghäuser 2023; Srivastava and Roy 2023). Globally, there have been enormous reports on the losses of properties worthy of millions of dollars and lives to flooding disasters (Islam and Wang 2024). On average, the global community recorded annual economic losses of 40 billion euros to flooding events in 2009 (Gaume et al. 2009). Additionally, in 2022, 176 flood disasters were recorded while between 2002 and 2021, 168 flood disasters were recorded at an estimated economic loss of $ 44.6 billion and 41.6 billion, respectively (CRED 2023). The higher record of floods in 2022 as compared to the two (2) decades (2002 to 2021), confirmed the worldwide ever increasing rate of flood occurrence.

Further evidence showed that flood disasters have been rated as one of the leading natural disasters in African countries, with severe rainfalls as the major cause (CRED 2019; Ahadzie et al. 2021; Alimi et al. 2022; Danso et al. 2024). Within the period of 19 years (1994—2013), Africa economically lost $ 912 billion to floods (UNISDR 2015). Approximately, 12 per cent of Africans experienced food insecurity caused by flood events between 2009 and 2020 (Reed et al. 2022). Flood events between 2010 and 2019, also accounted for 64 per cent of natural disasters in the continent (CRED 2019). Subsequently, parts of Africa experienced food insecurity, after crops were washed off by floods in 2022 (WMO 2022). As of December 2022, the United Nations Office for the Coordination of Humanitarian Affairs report for the year (2022) indicated; a death toll of 1418, while 4398 citizens suffered various degrees of injuries, and 2.9 million were also displaced in West and Central Africa (OCHA 2022). Flooding was ranked 56% of natural disasters in Africa with 43% of fatalities and 92% of economic losses (WMO 2022). Additionally, Tramblay et al. (2022) analysis of 13,815 historical flood records (1981–2018, 37 years) across Africa showed that 75% of them occurred as a result of intensive rainfalls. These further confirmed the perennial increasing rate of floods in Africa as a result of heavy rainfalls (Alimi et al. 2022) and it is therefore paramount for more studies to understand the mechanism of flood occurrences.

In Ghana, perennial flood disasters have been a national challenge, especially in the major cities, rural areas, communities, and cities within low-lying areas and or along river channels of the country (Dekongmen et al. 2021; Yin et al. 2021). Rapid rural–urban and urbanization have been accelerating these challenges through, unapproved settlements on waterways, paved surface areas, and poor waste management in Ghana, at the expense of potential flooding areas, thereby exposing many citizens to perennial flood disasters (Danso et al. 2024). However, in the rural areas, it is mostly the farmers who suffer the consequence of floods due to their predominant farming of rice and some water-like crop in low-lying areas, wetlands, and valleys (Smits et al. 2024). This confirmed that the frequency and severity of floods and other natural disasters increase as economic development and population densities encroach on these highly disaster risky zones (UNISDR 2015). In Ghana, flood disasters have been ranked as the highest natural disasters with a statistical representation of 32% from 2010 – 2019 (Kelly and Addo 2023). According to the Emergency Events Database (EM-DAT) from 1968 – 2023, floods accounted for 534 deaths and affected over 5,062,732 citizens within various parts of the country. The lower part of the Volta Basin of Ghana is yet to recover from 2023 floods that rendered many citizens along the basin homeless (IFRC 2023a). However, heavy rains are expected to worsen extreme floods in Ghana at a yearly projected cost of $ 160 million (The World Bank Group 2021).

The perennial flood cases in the major cities in Ghana have led to severally flood studies (Amoako and Boamah 2014; Frimpong 2014; Asumadu-Sarkodie et al. 2015; Twum and Abubakari 2019; Kordie et al. 2020; Osei et al. 2021a, b; Yin et al. 2021; Yin et al. 2022; Twum and Abubakari 2019; Osei et al. 2021a, b; Danso et al. 2024). However, none of such studies have been conducted in the Upper West Region (UWR) of Ghana. Worryingly, within the past decades, several episodes of these flood events have occurred in the UWR; a report from the EM-DAT indicated 52 losses of lives, with 29 injuries, 291,573 affected people, and home damages recorded at 33,000 in September 1999. National Disaster Management Organization (NADMO) records from 2016 to 2020 in the UWR, reported 553.5 acres of crop losses, and an affected population of 9,385, with an estimated cost of damage of Ghc 1,458,872.5. The most unbearable floods in 2021 (Fig. 1), led to massive unexpected destruction of homes, farms, roads, and even loss of lives. Shockingly, perennial spillages of excess water from the Bagre Dam in Burkina Faso coupled with extreme rainfalls are causing humanitarian challenges in the UWR and other Upper Regions of the country (Armah et al. 2010; Smits et al. 2024). These perennial floods have the potential to heighten food insecurity and disease outbreaks (Andrade

Fig. 1 Examples of flood disasters in 2021 in the region (**a**) Road washed off; **b** Daffiama-Sanwie Road; **c** Nadwoli –Wa Road; **d** Truck en route to Burkina Faso (Source: Ministry of Roads and Highways Ghana)

et al. 2018; Iqbal et al. 2022; Rehan et al. 2023; Ayenew and Kebede 2023).

Improving the situation in the region requires the provision of flood risk terrains information, which is crucial to support stakeholders in developmental planning, policy and decision-making, that will prevent urban dwellers from building on waterways. However, in recent years advanced datasets and methods; modelling approaches and techniques have evolved around the globe for conducting flood studies. These methods include but are not limited to analytical hierarchy process (AHP) and Geographic Information System (GIS) (Danumah et al. 2016; Cabrera and Lee 2019; Swain et al. 2020a, b; Ozturk and Safety 2021; Ramkar and Yadav 2021; Wicaksono et al. 2021), Artificial Neural Network (ANN) and Machine Learning (ML) (Adel et al. 2014; Sayers et al. 2014; Dazzi et al. 2021; Tamiru and Wagari 2022), Artificial Intelligence (AI) (Riazi et al. 2023), soil and water assessment tool (SWAT) and HEC-RAS (Ogras and Onen 2020; Taraky et al. 2021), GIS and Remote Sensing (RS) (Osei et al. 2021a, b), Frequency Ratio model, Fuzzy Logic (FL) Model, regional flood frequency analysis (RFFA) (Komi et al. 2016; Forson et al. 2023; Debnath et al. 2024), Watershed Modelling System (Soussa et al. 2012), and hydrological model (HEC-HMS) and Hydraulic model (HEC-RAS) (Tripathi et al. 2014; Shaikh et al. 2023; Al-Areeq et al. 2023; Baci et al. 2024). However, most of

these methods are often data and situational dependent and are mostly expensive to implement in developing countries (Samela et al. 2020).

Evaluating the complete possibility of stopping floods from occurring perennially may be artificially or naturally unachievable and elusive. However, the delineation of flood risk terrains is critical for flood adaptation, mitigation management, and sustainable development in the Upper West Region due to the perennial flooding. Therefore, this study, employed techniques such as; Jenks natural breaks classification (JNBC), and an integrated Geographic Information System (GIS)-based Analytical Hierarchy Process Multi-Criteria Decision (AHP-MCD) to delineate flood risk terrains, buffer zoning of communities along rivers/streams, evaluate historical flood records and population trends. Spatial distribution of rainfalls from 1992 to 2022 using Climate Hazards Group InfraRed Precipitation with Station data (CHIRPS) (Funk et al. 2015) was also visualized in a Jupyter notebook. Historical flood events data were also analysed to ascertain the trends of flood disasters in the region. The findings would set the ground for the development of a paradigm shift in policy that supports sustainable flood risk adaptations and mitigation measures, and water resources management in the region. This study is aligned with several studies conducted around the globe (Danumah et al. 2016; Swain et al. 2020a, b; Gupta and Dixit 2022; Nsangou et al. 2022; Shekar and Mathew 2023a, b; Ziwei et al. 2023).

Materials and method

Study area

This study focuses on the Upper West Region (UWR), Ghana, which is within longitude 1 25'' W and 2 45'' W and latitudes 9 30'' N and 11 N, and it shares a boundary with the Savanna Region to the south, with Upper East Region and North East Region to the east, with Burkina Faso to the north and the west with Cote d'Ivoire (GSS 2013; Baddianaah et al. 2022). The region has total land coverage of 18,779.71 square kilometres (Fig. 2) and it comprises about 12.7% of the total landmass of the country. The agroecological zone of the region is within the Guinea Savannah and Sudan Savannah belt (Diabene et al. 2014) with common trees such as; dawadawa, manula, shea, baobab and neem. These trees provide economic value to the people as well as firewood for domestic use. Generally, the most cultivated crops in the Upper West include; nuts, tubers, vegetables and cereals (Diabene et al. 2014). Currently, the region has a population of 904, 695, which constitutes 2.9% of the total

population of Ghana (GSS 2021). The region experiences continental tropical air masses (dry and hot) (Brulard 2011). It experiences a single rainy season, lasting for a period of 4 to 5 months (April to September), with an annual average rainfall ranging from 840 to 1400 mm. The rainfall tends to be heavy between August and September. The northeast trade winds which bring the dry season known as the 'harmattan' start at the recedes of the rainy period, and are characterized by cold and hazy weather conditions from November to March, hot weather conditions, which only seize at the onset of the rainy season. Temperatures in the region are generally high; with monthly mean temperatures ranging from 21 to 32 °C, which rise to about 40 °C somewhere in March—April and fall to 20 °C in December (GSS 2013;Saana et al. 2016; Abu et al. 2024). The topography of the region is almost gently flat with Lawra and the western part of Wa mostly referred to as the Wa-Lawra plains, with a height of land range between 250 and 300 m. The western part of the region is drained by the Black Volta River Basin (BVRB), while the central and eastern parts of the region are drained by the Red and White River Basins (Kulpawn
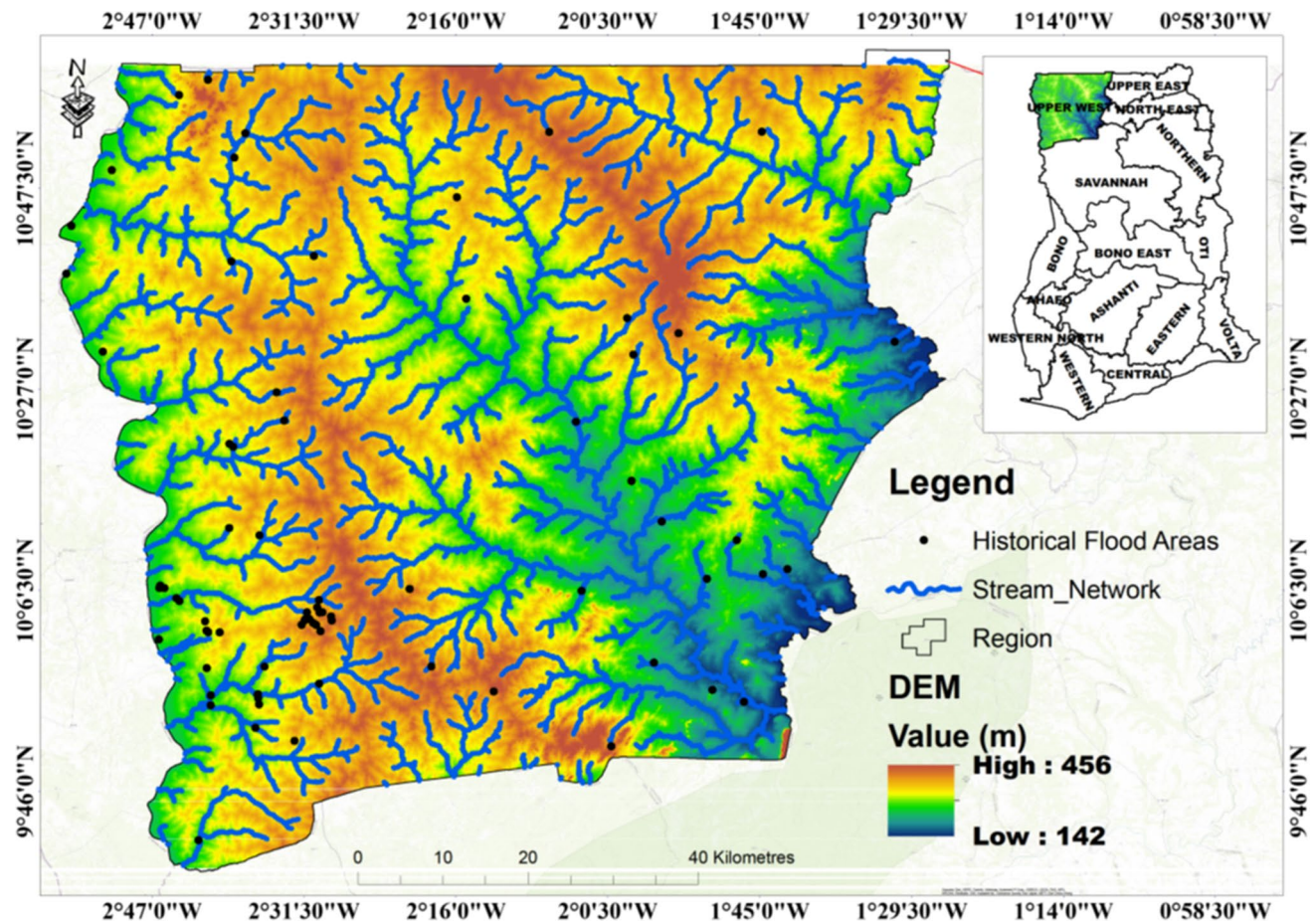

Fig. 2 Study area (UWR) map

River and Sisili River), with their various tributaries from the sub-catchments are discharging southwards into the White Volta River Basin in the southern. Soil structure, texture, porosity, coarse nature, clay composition, and organic matter control the permeability and water holding capacity (Ball 2011; Kerr et al. 2016; Irvin IV et al. 2023). However, the soil types found in the region were Acrisols, Arenosols, Fluvisols, Leptosols, Lixisols, Planosols, Plinthosols, and Vertisols. These soils are largely generated over granite with some fewer areas developed over lower Birimian phyllite. The geology features Basal Sandstone, Birimian Sediments, Birimian Volcanics, Dahomeyan, Obosum and Oti Beds, and Upper Voltaian (Abdul-Ganiyu and Kpiebaya 2020).

Methods

To spatially delineate flood risk terrains over a watershed, topographical and or hydrological surfaces to support policy and decision-making requires datasets and tools. Succinctly, the details of each data and method of analysis employed in this study have been explicitly described in the sub-sections of the study. Figure 3 summarises the insightful steps employed in conducting this study. However, the flood risk

terrain maps were developed using two techniques; Jenks natural breaks classification (JNBC) and GIS-based AHP-MCD. Jenks' natural breaks classification (JNBC) (Jenks 1967; Guoyi et al. 2023) technique was employed to first optimize the delineation of the five (5) classes of the study area, to initially demarcate flood-susceptible areas within the study area, which provided an insight into the flood risk terrain to be expecting. JNBC techniques algorithm has been employed in conducting flood hazard studies and other studies (Anchang et al. 2016; Toosi et al. 2019; Amirruddin et al. 2020; Mishra and Sinha 2020; Deroliya et al. 2022). This algorithm ensures the optimal arrangement of classes' values within a group and between classes. JNBC optimization determines to reduce the intra-class means deviation while ensuring that the inter-class means are maximized (Jenks 1967). Each of the classes indicates an area within the study area that would likely suffer perennial floods during heavy rainy days or periods, as a result of a high volume of surface runoff inundation due to the heavy rainfalls (Toosi et al. 2019). There have been enough shreds of evidence of heavy rainfalls as the cause of severe flood disasters in the Upper West Region (UWR) (IFRC 2023b), as a result, Jupyter notebook was employed to visualize Climate Hazards
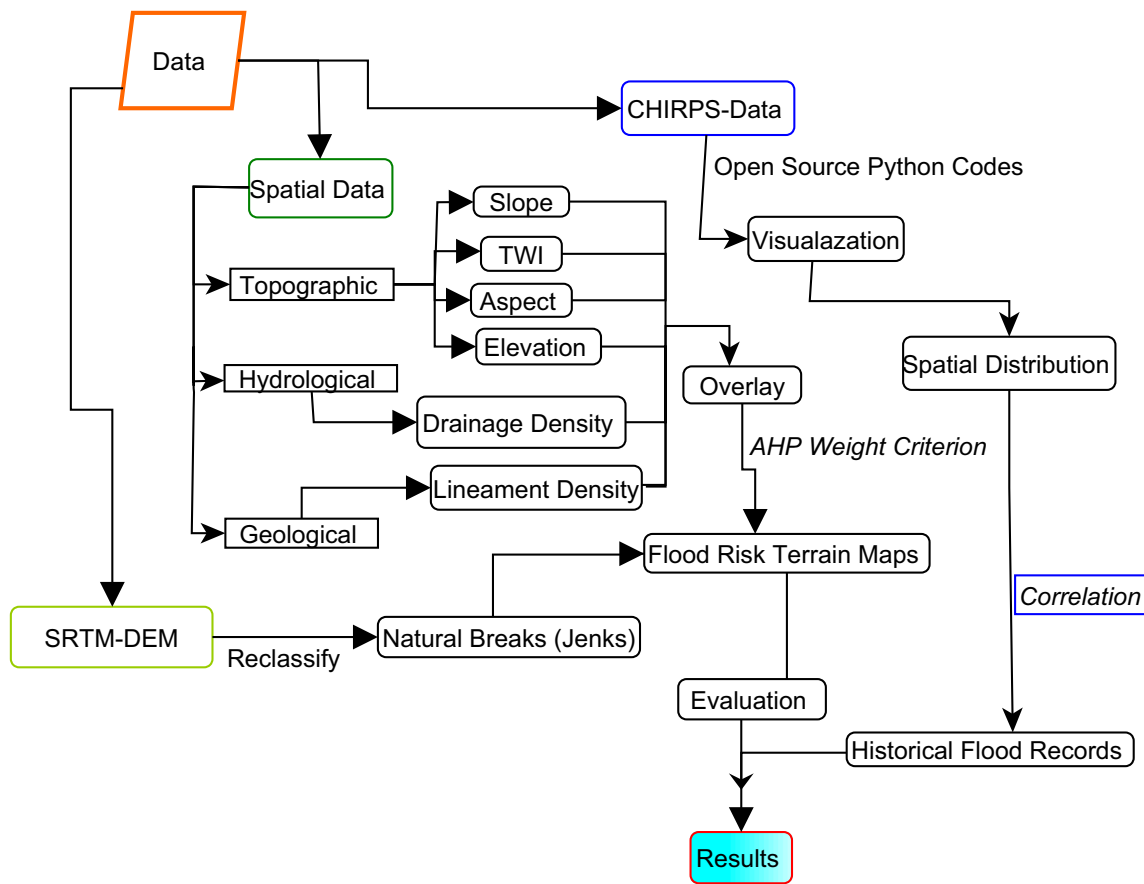

Fig. 3 Flowchart of the study process

Group InfraRed Precipitation with Station data (CHIRPS) (Funk et al. 2015) for 30 years (1992 to 2022). The average monthly and August rainfall events were visualized. In addition, the study analysed population growth and historical flood events in the study area to understand their trends. Most especially, a correlation matrix of rainfalls and flood events records was also carried out.

Data acquisition

Historical flood records give a preliminary knowledge of present and future floods in a catchment. Therefore, in this study, both primary and secondary datasets from various sources including local departments and organizations were collected and used. Secondary data on historical flood disaster records from 2016 to 2021 were sourced from the Upper West Regional National Disaster Management Organization (NADMO). Population growth rate is a key factor in exposure to flood vulnerability (Nguyen et al. 2021). As a result, population data between 2010 and 2021 was also obtained from the regional Ghana Statistical Service (GSS) department, Wa, Ghana. These datasets were sourced to explore the trend of floods and population growth within the UWR. However, there are no generally accepted methods and techniques for classifying flood potential areas, delineation fo flood risk terrains, flood zoning etc. (Jodhani et al. 2021), as there are several methods and factors that influence flood occurrences (Bello and Ogedegbe 2015). Al-Areeq et al. (2023) noted a better performance of the 30 m Shuttle Radar Topographic Mission (SRTM) DEM in flood extend assessment as compared with 12.5 m ALOSPALSAR, 10 m Sentinel 1, 30 m Advanced Spaceborne Thermal Emission and Reflection Radiometer (ASTER) and 90 m MERIT products. Therefore, to develop a spatial flood risk terrain (FRT) map of the UWR, the SRTM DEM from USGS was used to generate the various thematic maps. Woeful, the paucity of data in the region to model the hydrological and hydraulic dynamics in the region has prevented innovative modelling of early warning systems and designs. After carefully reviewing the literature (Okyere et al. 2013; Arabameri et al. 2018; Al-Areeq et al. 2023; Shekar and Mathew 2023a, b; Shekar and Mathew 2023a, b; Ahmed et al. 2024; Danso et al. 2024; Jemai et al. 2024), six (6) spatial topographical, hydrological, and geological flood conditioning sub-thematic factors comprising topographic wetness index (TWI), Drainage Density (DD), Elevation, Slope, Lineament Density (LD), and Aspect, were selected based on the data availability, and the nature of the UWR topography to explore areas susceptible to flood disasters. These spatial thematic factors selected, significantly control landscape forms and characteristics, and hydrological processes, that drive surface runoff (Danumah et al. 2016; Ahmad 2018; Toosi et al. 2019; Mishra and Sinha 2020; Karymbalis et al.

2021; Leandro and Shucksmith 2021; Addis 2022; Amen et al. 2023). As a result, several, studies conducted around the globe selectively combined different thematic factors to either model, delineate, and assess; flood risk areas (Liuzzo et al. 2019; Mishra and Sinha 2020; Swain et al. 2020a, b; Roy et al. 2021; Gacu et al. 2022; Al-Taani et al. 2023), and groundwater recharge potential zones (Andualem and Demeke 2019; Gómez-Escalonilla et al. 2022; El Ayady et al. 2023; Ishola et al. 2023; Kumar et al. 2023; Moharir et al. 2023; Shekar and Mathew 2023a, b; Tariq et al. 2023; Feujio et al. 2024), soil erosion (Ahmad 2018) and landslides (Poddar and Roy 2024), indicating that flood modelling or assessment is not static to one set of datasets. Ground truthing points (GTPs) of some historical and frequent flooding points were collected from the field with a GPS device. The CHIRPS from Digital Earth Africa sandbox (https://sandbox.digitalearth.africa/) were also analysed to highlight the trend of the spatial distribution of the rainfall behviour during the flood seasons over the UWR. However, buffer zoning was also employed to capture communities likely to be inundated when the streams and rivers flow their banks during peak rainy seasons.

Preparing and comparing flood-causing Sub-thematic factors

After establishing the sub-thematic factors preparation, the Saaty method (Saaty 1977) of Analytical Hierarchy Process (AHP)-Multi-Criteria Decision (MCD) (AHP-MCD) which has been applied in several flood studies (Danumah et al. 2016; Cabrera and Lee 2019; Swain et al. 2020a, b; Gacu et al. 2022; Gupta and Dixit 2022; Al-Taani et al. 2023; Shekar and Mathew 2023a, b) was used to rank these factors through assigned weighted values based on their strong relative relevance and contributing to runoff inundation, overland flows, and flood risk within the territory (Amen et al. 2023). AHP-MCD was done through a pair-wise comparison matrix of the sub-thematic factors, based on an expert judgement and knowledge of the research terrain, on how the factors are influencing flood within the area (Gacu et al. 2022). The consistency of each sub-thematical factor was assessed to ensure they were consistent with each other or not, using Eqs. 1 and 2.

$$CI = \frac{\lambda_{max-n}}{n-1} \tag{1}$$

$$CR = \frac{CI}{RI} \tag{2}$$

CR, CI, RI (Table 1), and λ_{max} represent the consistency ratio, consistency index, random index, and matrix principal eigenvalue respectively. However, n (Table 1) also

presents the number of sub-thematic factors being compared (Abdrabo et al. 2023; Ahmed et al. 2024).

The consistency ratio (CR) for a 3×3 matrix and a 4×4 matrix are 0.05 and 0.09, respectively. CR of 10% (0.01) in general, is for large matrices. The computed CI from the process was found as 6.254, which yielded a computed CR value of 0.04 for the six factors (n = 6, RI = 1.25), which is less than 0.01. The CR value calculated was within the acceptable range and it, therefore, indicated that the pairwise matrices were consistent with each other (Gupta and Dixit 2022). Table 2 presents the environment's natural hydrological, geological, and topographical sub-thematic conditioning factors of floods. The rating of each sub-thematic factor's class weight was determined by the Saaty, (1977, 2004) scale of 1 to 9. The scale values range from equally importance through to extremely important (see Saaty 1977). Therefore, classes that were adjudged as equally important

and extremely important were assigned values as 1 and 9 respectively. For Saaty's scale from 1 to 9 of the intensity of importance see (Saaty 1977, 2002, 2004). The AHP-MCD weightage values for all the sub-thematic factors; Drainage density, elevation, slope, lineament density, TWI, and aspect, were 0.27, 0.17, 0.09. 0.21 and 0.05, respectively (Table 2). The sub-thematic factors were integrated and overlaid to generate the final AHP-MCD map.

Lineament density

Lineaments are geological features such as faults, fractures, joints, streams and valley networks (Das 2017; Das and Pardeshi 2017; Slimani et al. 2023; Tegegne et al. 2024). The sum of the length of all lineaments (Li) over an area is known as the lineament density (L_D). L_D regulates the flow of both surface runoff and groundwater by serving as

Table 1 Standard values of random index (RI) (Donegan and Dodd 1991; Saaty 2002, 2004)

N	0	2	3	4	5	6	7	8	9	10	11
RI	0.00	0.00	0.52	0.89	1.11	1.25	1.35	1.40	1.45	1.49	1.51

Table 2 Weightage assignment of each factor

Flood Causative Criterion	Unit	Class	Susceptibility Class Ranges and Ratings	Susceptibility Class Ratings	Weight (%)
Drainage Density (DD)	km/km^2	0–11.75	Very Low	1	27
		11.75–23.50	Low	2	
		23.50–35.26	Medium	3	
		35.26–47.01	High	4	
		47.01–58.76	Very High	5	
Elevation	m	150–200	Very High	5	21
		200–250	High	4	
		250–300	Medium	3	
		300–350	Low	2	
		350–400	Very Low	1	
Slope	%	0–1.73	Very High	5	17
		1.73–3.213	High	4	
		3.214–6.919	Medium	3	
		6.9216.56	Low	2	
		16.57–63.02	Very Low	1	
Lineament Density (LD)	km/km^2	0–12.71	Very Low	1	9
		12.71–20.25	Low	2	
		20.25–27.15	Medium	3	
		27.15–34.47	High	4	
		34.47–54.94	Very High	5	
Topographic Wetness Index (TWI)	Level	-6.58-, -2.57	Very Low	1	21
		-2.56-, -0.999	Low	2	
		-0.999-, -1.2	Medium	3	
		1.2–4.51	High	4	
		4.51–13.5	Very High	5	
Aspect	Direction	-1–71.13	Very High	5	5
		71.13–143.26	High	4	100
		143.26–215.38	Medium	3	
		215.38–287.51	Low	2	
		287.51–359.64	Very Low	1	

conduits (Slimani et al. 2023; Tegegne et al. 2024). There-fore, the lineament networks were first extracted from the DEM in a Geomatic PCI environment. The lineament density was further generated using the Line Density based on Eq. 3 and reclassified into five classes ranging from 0–54.94 (Fig. 4a) in the GIS tool environment.

$$L_D(\text{Lineament Density}) = \Sigma \, Li/_A \qquad (3)$$

where Li is the sum of the length of lineaments in m or km and A is equal to the area (m^2 or km^2).

Elevation

Elevation influences the speed and flow direction of sur-face runoff rate, which encourages terrain susceptibility to flood risk. Terrains with low elevations, low-lying and flat slopes have a high risk of perennial flood occurrences. The elevation is, therefore, vital in determining flood risk terrains (Association of State Floodplain Managers 2020). Surface runoff moves from high lands to low lands; flat and lower terrains are more than susceptible to flood hazards (Shekar and Mathew 2023a, b) due to the rapid inundation of water. The elevation of the study area was extracted from the national elevation shapefile and reclassified into five classes ranging from 150 to 400 m (Fig. 4b).

Topographic wetness index

The Topographic Wetness Index (TWI) is an important flood conditioning characteristic factor in flood risk terrain map-ping. TWI regulates surface runoff accumulation tendency within a point in a watershed, and the soil wetness or dry-ness, saturation, moisture, and water depth (Costache 2019; Chowdhuri et al. 2020). A terrain with lower TWI values indicates that it is less prone to perennial flood risk (Shekar and Mathew 2023a, b), while high TWI values are con-sidered high-risk flood vulnerability (Rahman et al. 2023) because saturated soil influences overland flows leading to inundation (Shekar and Mathew 2023a, b). DEM was used to generate the TWI map using Eq. 4;
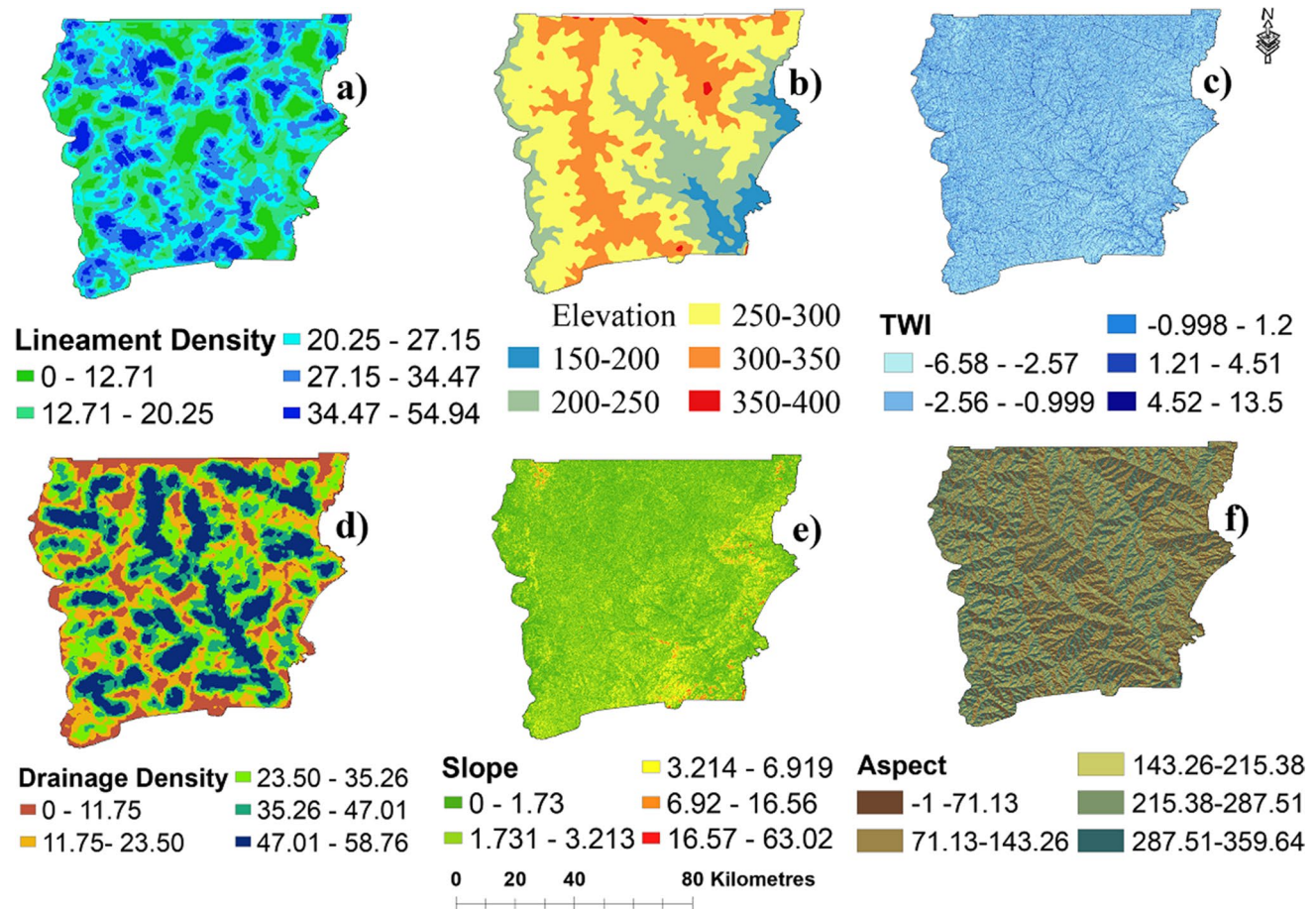

Fig. 4 Spatial thematic factors influencing flood risk terrains in the UWR: **a** Lineament Density(km/km^2), **b** Elevation (m), **c** TWI, **d** Drainage Density (km/km^2), **e** Slope (%), and **f** Aspect (degree)

$$TWI = \frac{In(As)}{Tan\beta} \qquad (4)$$

As and β are the upstream area (area/length_m2/m) and slope gradient (degrees) of the watershed respectively (Das 2019) Paul et al. 2019; Rahman et al. 2023). The generated TWI map was reclassified into five classes ranging from -0.99 – 13.5 (Fig. 4c).

Drainage density

The drainage density (DD) forms the runoff connectivity patterns of the study area. It is the summation of the streams and rivers' length within a watershed/catchment divided by the total area of the basin (Rahman et al. 2023). Terrains with high DD values are highly susceptible to floods as well and terrains with lower DD are less prevalent (Getahun and Gebre 2015; Rahman et al. 2023; Shekar and Mathew 2023a, b; Kannapiran and Bhaskar 2024). To generate the DD, rivers/stream networks were first generated from the DEM and were used via the Line Density tool in the GIS tool under the Spatial Analyst tool. The generated DD was further reclassified into five (5) classes (Fig. 4d) ranging from low (less DD) to high (denser DD) (0 – 58.76 km/m2) using Eq. 5 below.

$$\text{Drainage Density(DD)} = \Sigma\ {}_{Lr/_A} \qquad (5)$$

L_r is the total length of rivers and streams, while A is the total area of the watershed or catchment of the study area.

Slope

The slope is a major conditioning factor in spatial flood risk terrain identification (Karymbalis et al. 2021; Osei et al. 2021a, b; Ayenew and Kebede 2023). And how slope characteristics define the nature of an area's extreme rains is critical. As a result, slope angles are important features in hydrological process modelling. It is a driving force of surface runoff and flow accumulation (Costache et al. 2021) that influences infiltration and soil erosion (Rahman et al. 2023) and high speedy runoff in high-land and waterlogging/flood inundation within low-lying terrains (Sachdeva and Kumar 2022). Generally, slope angles are important features in hydrological process modelling. Terrains within flat and low slope gradients are highly susceptible to the risk of flood while areas with higher sloppy terrain are less susceptible to flood (Liuzzo et al. 2019). To extract the slope of the study area, raster data of the digital elevation model (DEM) was used as an input. The region of interest (ROI) shape file was used as the boundary to digitize the DEM for the study. The spatial analyst tool in the GIS tool toolbox generated the slope from the DEM by calculating the maximum rate of changes in angle between each cell and its neighbour's cell. The slope was calculated in per cent of the slope based on Eq. 6.

$$\text{Degree of slope} = \theta, \text{percent of slope} = \frac{\text{Rise(Height)}}{\text{Run(Length)}} \times 100 \qquad (6)$$

The produced slope map was reclassified into five classes ranging from 0–63.02% (Fig. 4e). Different colour codes were selected to designate areas liable to high and low flood occurrences. Red colour codes were assigned to areas with a high degree of susceptibility to flood occurrences. Green colour codes designated areas with moderate vulnerability of flooding and lower flood susceptibility were also assigned with yellow colour codes.

Aspect

Aspect shows the directions at which a slope is facing (Yu et al. 2023a, b). Aspect is measured in a clockwise direction in positive degrees ranging from 0 – 360, however, areas with zero or flat slopes are assigned negative ones (-1). The zero or flat aspects of terrains are the driving force of rapid surface runoff direction and accumulation, likely to result in floods (Sachdeva and Kumar 2022). DEM was used to generate the Aspect for the UWR, using the Surface tool in the GIS tool. The Aspect map was then reclassified into five classes ranging from -1 – 359.64 (Fig. 4f).

Population data

Equation 7 was applied in computing the population growth rate of the study;

$$R = \frac{[Nt - NO]}{N0} * 100 \qquad (7)$$

where: R = population growth rate, Nt = the final population size at time t, N0 = the initial population size at time 0.

Climate hazards group infrared precipitation with station data (CHIRPS)

The CHIRPS are satellite derived areal data average datasets, especially for rural, complex terrain and, semi-arid regions that are data-scared due to fewer rain gauge stations (Funk et al. 2015; Dinku et al. 2018). This was initiated through collaborative efforts with the United States Geological Survey Earth Resources Observation and Science (USGS-EROS) Centre to produce an up-to-date and complete reliable rainfall dataset for analyzing the trends and seasonal variations of the rainfall for monitoring and evaluation of hydrological occurrences, to support effective early warning systems development. The datasets have a record

of over 30 + years spanning from 1981–01 up to date, with a spatial resolution of 0.05^0 with an approximation of 5.55 kms (López-Bermeo et al. 2022). CHIRPS was chosen due to its better performance as compared to other satellite products in Ghana (Atiah et al. 2020). Atiah et al. (2020) validated satellite products with 113 observation stations data over Ghana where findings showed a strong agreement with observed rainfall data and CHIRPS data as compared to the other products. A strong correlation of over 0.9 between CHIRPS and observational station data was also observed in the Upper Savannah agroecological zone as compared with the other agroecological zones in Ghana (Atiah et al. 2020). Ayehu et al. (2018) and Dinku et al. (2018), also reported better performance of CHIRPS products in East Africa as compared to other satellite products, this further strengthened the use of CHIRPS data in areas with observed data scarcity.

This necessitates the use of 30 years (1992–2022) of CHIPRS data to spatially visualise rainfall in the study area, at various spatial distribution scales; annual averages, five (5) year annual averages, monthly averages, and the month of August for each year.

Evaluation of FRT maps

The findings from this study will not be scientifically valid for policy and decision-making, if not evaluated using historical flood events (Cabrera and Lee 2019; Nsangou et al. 2022; Santosa et al. 2022; Upadhyay et al. 2022). Therefore, to ensure the reliability of the flood maps (both JNBC and AHP maps), ground truthing points (GTPs) of 85 historical flood points were collected within the study (Upper West Region (UWR)) after the 2021 direful flood events. The GTPs were overlaid on the maps and clipped to each class of the maps, to identify the number of points that were captured within each class. The captured points within each class were then calculated as per cent of the total points. Though there are several accuracy techniques such as; the area under receiver operation characteristic (ROC) curve known as AUC (Wang et al.2019; Arabameri et al. 2020; Pham et al. 2021; Rahman et al. 2021; Roy et al. 2021; Wubalem et al. 2021; Ghosh et al. 2022; Kumar et al. 2023; Shekar and Mathew 2023a, b; Tariq et al. 2023) for evaluating flood risk terrains, flooding areas, and potential zones delineation, however, application of this validation method was based on scientific studies and practices (Molinari et al. 2019; Amen et al. 2023). This is also imperative because, the methods presented have the potential to delineate FRTs and illustrate sensitive flood information to support flood mitigation strategies within the catchment, and therefore the findings have to be evaluated to ensure reliability and validity to boost the confidence of decision-makers (Molinari et al.

2019; Leandro and Shucksmith 2021; Addis 2022; Al-Taani et al. 2023).

Results and discussion

Flood risk terrains analysis

The JNBC algorithm optimized the study area into five (5) classes of flood risk terrains (FRTs) as illustrated in Figs. 5a and 6. The five classes were calculated as 4% (856.278 km²), 7% (1466.685 km²), 12% (2418.642 km²), 35% (7014.96 km²), and 42% (8351.496 km²) representing; very high, high, moderate, low, and very low FRTs, respectively. The very high and high flood risk terrain classes were observed along the southeastern and eastern parts of the study area, that is within the Sissala East Municipality (SEM) and Wa East (WE) district of the region, which agreed with the low elevation and low slope nature of the terrains. These findings were consistent with other studies that asserted the high chances of extreme flood occurrences in low-lying areas (Das 2019; Ullah and Zhang 2020; Al-Taani et al. 2023). The moderate and low risk terrains were also observed along the patterns of the very high and high flood risk terrains and the western border of the Black Volta River Basin (BVRB). More illustrations showed that the low and moderate risk terrains dominated within five districts; Jirapa, Lawra, Nadowli-Kaleo, Nandom, and Wa West, which share borders with the BVRB. Further observation showed that the very high and high flood risk terrains within the southeastern and eastern part of the study area are along the major rivers; Kulpawn and Sisili banks, this affirms that floods are ever occurring along river conveyances (Sofia and Nikolopoulos 2020). The areas along the river banks also have gentle to flat slope terrains, that is low elevations and low slopes which are attributed to high susceptibility to flood risks and similarly were observed by Ullah and Zhang (2020) along the Panjkora's river banks. This also underpins the fact that the gentle to flat nature of the study area is generally influenced by overland flows during peak rainy seasons, leading to the high records of perennial floods. This further bears out the frequent flood occurrences within low-lying areas in the study area. Therefore, the knowledge of the terrain behaviour is paramount to the rice farmers and stakeholders' economic activities (Nguyen et al. 2021) of their proximity to these vulnerable areas. Assertively, other studies attest the closeness of communities and citizens to and within these vulnerable areas facilitates frequent flood hazards (Nazeer and Bork 2021; Mwalwimba et al. 2024).

The GIS-based AHP-MCD approach was also employed in weighing and comparing the sub-thematic flood conditioning factors, and integrating and overlaying the factors over each other generated the final FRTs map (Das 2019;

Fig. 5 Flood risk terrains: **a** Natural Breaks (Jenks) method and **b** AHP-MCD method
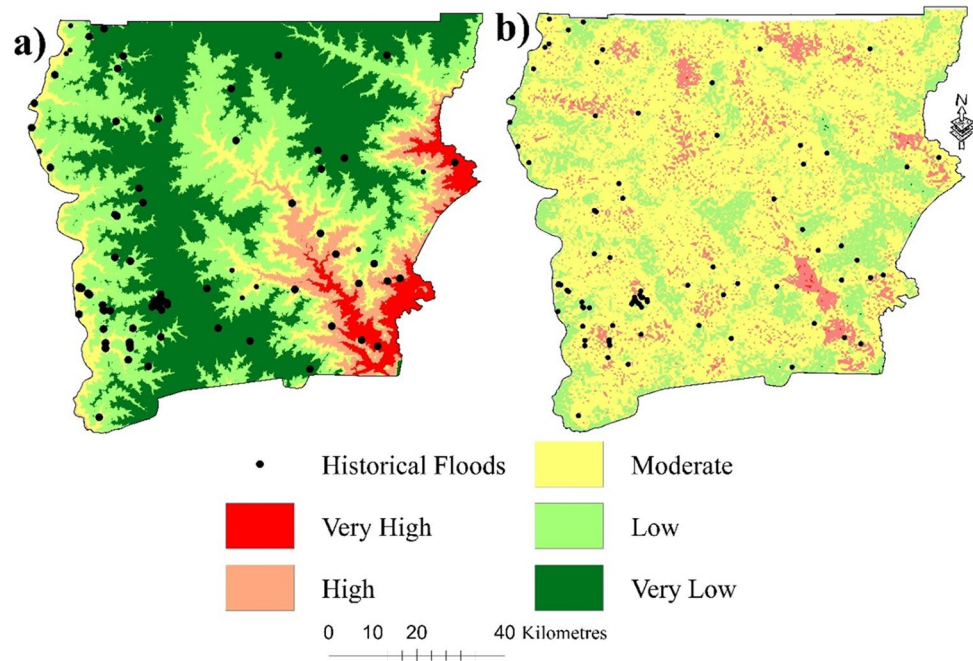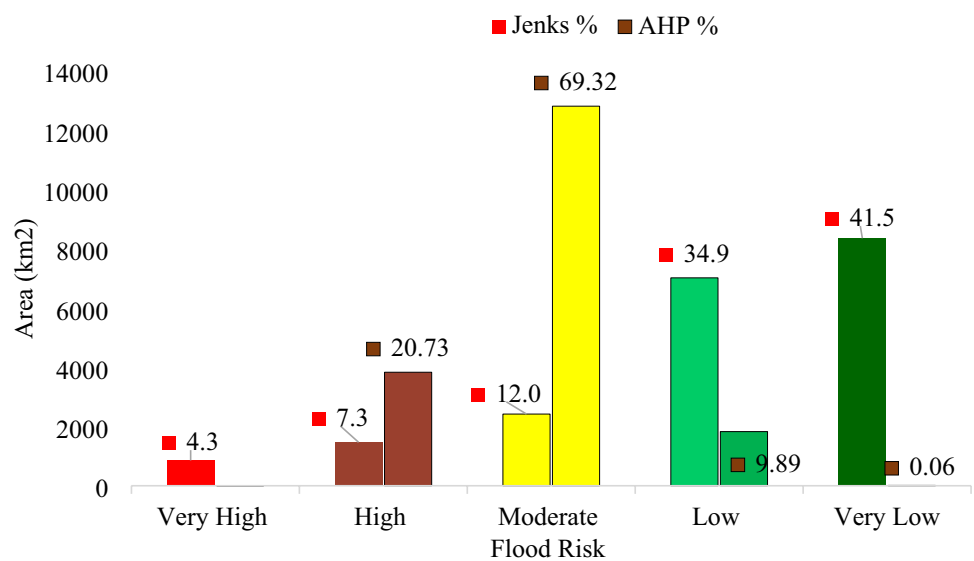

Fig. 6 Flood risk terrains; Natural Breaks (Jenks) method and AHP method

Liuzzo et al. 2019; Toosi et al. 2019; Wang et al. 2019; Ullah and Zhang 2020; Addis 2022; Al-Taani et al. 2023; Shekar and Mathew 2023a, b; Suwanno et al. 2023). The final output map was classified into five (5) categories of flood risk terrains, ranging from very high to very low. This was done based on the susceptibility of each class to flood occurrences. Figure 5b illustrates the spatial distribution of the FRTs over the study area, while Fig. 6 presents the FRTs in percentages. The five categorised classes were namely; very high, high, moderate, low, and very low with areas coverage of 0.707 km^2 (0.004%), 3830.02 km^2 (21%), 12,807.31 km^2 (69%), 1827.011 km^2 (10%), and 11.535 km^2 (0.062%)

respectively. Figure 5b shows that the majority of very high and high flood risk terrains are spatially distributed along the southeastern, eastern and north, while some are sparsely scattered within the whole region. This could result in scattering of extreme flood disasters over the region (UWR) since they are not confined to a specific location. Further observations clearly showed that the very high and high FRTs are heavily found along the stream/river networks, confirming that low-lying areas are susceptible to flood disasters (Pham et al. 2021; Amen et al. 2023; Shekar and Mathew 2023a, b; Danso et al. 2024). These findings were also consistent with a study by Rana et al. (2023). Additionally, the

very high and high FRTs also coincided with the flat to low slope, low elevation (150–300 m), high drainage density (47.01–58.76 km²/km), and high TWI (4.52–13.5), which influence the high accumulation of runoff during rains. This also confirms that the topography plays a major role in conditioning flood susceptibility in low-lying terrains. The very low and low FRTs are found in areas with higher slopes, higher elevations, and low drainage density, especially, within the highland areas in the region. The moderate FRTs were discovered as the dominant class, spatially distributed all over the study area, and accounted for 69 per cent of the total study area. Furthermore, critical observations also noted that the majority of the very high and high FRTs are sandwiched within the major river catchments (Kulpawn River and its tributaries) and alongside the Sisili River in the region. This indicates that the communities, districts, and farms are in perennial flood danger during the rainy periods. This has also been verified by the historical perennial flood events in some communities and districts in the region. That is, those communities, districts, and municipalities which are heavily drained by the Kulpawn River and Sisili River and their minor tributaries during rainy seasons; most especially Wa East, Sissala East, Sissala West, Daffiama Bussie Issa and the eastern part of Jirapa. This revealed that low-lying areas, most especially those along the rivers/streams are risky zones, due to overflows of their banks. However, due to the nature of agricultural activities in the region, farmers mostly plant crops such as rice within low-lying; waterlogs, waterways, valleys, rivers/streams banks, and near dugouts' areas, and this increases the perennial exposure of the farms to flooding, inundate and washing away of crops. The results from this study, significantly affirm that the very high and high FRTs in the study area are not homogeneous, and are distributed all over the region. This is also sign that the moderate FRTs are likely to experience unprecedented extreme floods, due to spillover and overflows from the very high and high flood risky areas (Amen et al.2023). These observations, further confirmed Ghana's flood prone areas are always along rivers/streams, near rivers, waterways, poor drainage networks, encroachment of waterways, and river basin sites, which are often serving as high runoff retention areas (Okyere et al. 2013; Yin et al. 2021, 2022; Gaisie and Cobbinah 2023; IFRC 2023a).

The knowledge and information of flood vulnerability areas, risky terrains, flood drivers, and their impacts are key factors for strategic flood disaster management, policy, and decision-making (Nazeer and Bork 2019; Li et al. 2022). Delineation of flood risk terrains and flood studies are rare in this part of the country, despite the perennial flood disasters. However, apart from drought, flooding has been the most disastrous problem, affecting thousands of lives and properties. Hence, the study aims to scientifical delineate these flood risk terrains in the region in support of farmers,

stakeholders, and NGOs, and to boost sustainable developments in the region.

Validation of flood risk terrain maps

The ground truthing points (GTPs) of historical flood events were overlayed and clipped to each of the FRTs maps. The JNBC map classes recorded; 31.76% (very low), 16.47%, (low), 15.29% (moderate), 24.71% (high), and 11.76% (very high) flood risk terrains, respectively. Quantitatively, 31.76% of the flood historical points were recorded in the very low flood risk areas, while the very high-risk regions recorded the lowest points with 11.76%. The generation of the JNBC map did not take into consideration other flood influencing factors which limited its ability to delineate a truthful representation of flood occurring areas within the study area. During the field data collection, it was also observed that several communities, and suburbs within the Wa Municipality are encroaching on, and sandwiching stream/river networks within the city, which probably led to the 31.76% of GTPs within the very low class. During the evaluation of the AHP-MCD map reliability, it was observed that none of the GTPs was found within the very low and very high flood risk terrains classes. However, the low, moderate, and high classes recorded; 20%, 71.76%, and 8.24% of the GTPs, respectively. It is also arguable that the very low (11.54 km²) and very high (0.71 km²) risk terrains in terms of area were insignificant which could probably be the reason why no GTPs were found in their classes. The higher number of GTPs found within a class shows the susceptibility of that class to flood events (Toosi et al. 2019). Therefore, 71.76% of the historical flood events recorded within the moderate class, revealed that the study area (UWR) is largely dominated by moderate flood risk terrains. The validation also further showed that flood disasters are not homogeneous within the study area. This confirmed the reliability of the findings to assist and support stakeholders in flood planning, decision-making, and policy (Amen et al. 2023).

Buffer zoning of stream network

Buffer zoning (bz) plays a key role in regulating flood risks along streams and rivers (Osei et al. 2021a, b; Kurugama et al. 2023). During the heavy rainy seasons, most streams and rivers overflow their banks to some extent which provokes inundation and flooding communities and farms within their catchment. It is well noted that in most communities in the UWR, farms sandwich wetlands, along streams and valleys, and near dugouts (commonly called dams in the region). At the end of the 2021 flood disasters, NADMO reported 121 communities in some municipalities and districts (Sissala East Municipality (SEM), Sissala West Municipality (SWM), Wa East (WE), Wa West (WW),

Nadowli-Kaleo, Lawra, Lambussie/Karni, and Wa Municipality (WM)) in the region as flood risk communities. Therefore, to further identify the number of communities likely to experience fluvial floods in the UWR, a buffer zoning of the stream/river networks in the study area was, therefore, important to further observe the pregnant communities that would be inundated whenever these streams/rivers overflow their banks into their flood plains and their nearby subbasins. A buffer of 0.5 and 1 km was selected to observe communities likely to be inundated within the flood risk zones when rivers/streams overflow their banks. With about 1952 community points in the UWR, it was observed that 395 (Fig. 7a) and 927 (Fig. 7b) communities were found as sandwiched between 0. 5 km and 1 km respectively. It further revealed that these communities within the buffered ranges are sited within the moderate, high, and very high flood risky terrains (both JNBC and AHP-MCD maps). It is paramount to understand that these communities are more susceptible to high flood hazards than those outside the buffer zones. Notwithstanding the several flood conditioning factors; settlement encroachment on wetlands, heavy rains, waterways, low-lying areas, runoff retention areas/runoff converging points, rapid population growth etc. (Yang et al. 2022) and climate change impacts (IPCC 2023b). These findings were also consistent with Toosi et al. (2019) and Osei et al. (2021a, b) studies, which revealed that communities within the buffer zones are more prone to flood disasters than those outside the border. This further highlights a sign of future flood disaster severities in the informal urban settings and communities in many developing countries (Juma et al. 2023). As

it has already been reported, flood disasters in developing countries are expected to increase due to rapid infrastructure encroachment on waterways and climate change that owes its impact to severe rainfalls (Anwana and Owojori 2023; IPCC 2023a, b). Therefore, buffer zoning is a key component towards delineating retention zones for sustainable development and planning of cities and communities (Cabrera and Lee 2019; IPCC 2023a, b). However, there is an arguable assumption that cities' and communities' exposure to flooding disasters is constant as the population keeps increasing and settling around and near risky and vulnerable areas (Aerts et al. 2018; Tesselaar et al. 2023). These findings highlight the importance of integrating buffer zoning into the policy in the communities, towns and municipal planning.

Historical flood disasters in Upper West Region (UWR)

Figure 8 presents historical flood event records over six (6) consecutive years (2016–2021) from the National Disaster Management Organization (NADMO) in the UWR. The report indicated significant flood disaster experiences, which affected over 1,344, 6,806 and 6,190 people in 2016, 2018, and 2021, respectively. Floods in August 2021, were recorded as the worst disaster, that has ever happened in the region, with an estimated cost of 1,183,660.00 Ghana Cedis. It was also further observed that the affected population rose with the economic losses, especially in the years; 2016, 2018, and 2021, which were hard hit years. The statistics (Fig. 8) revealed that the population affected in 2018

Fig. 7 Buffer zoning (bz) communities: **a** communities within 0.5 km bz and **b** communities within 1 km bz
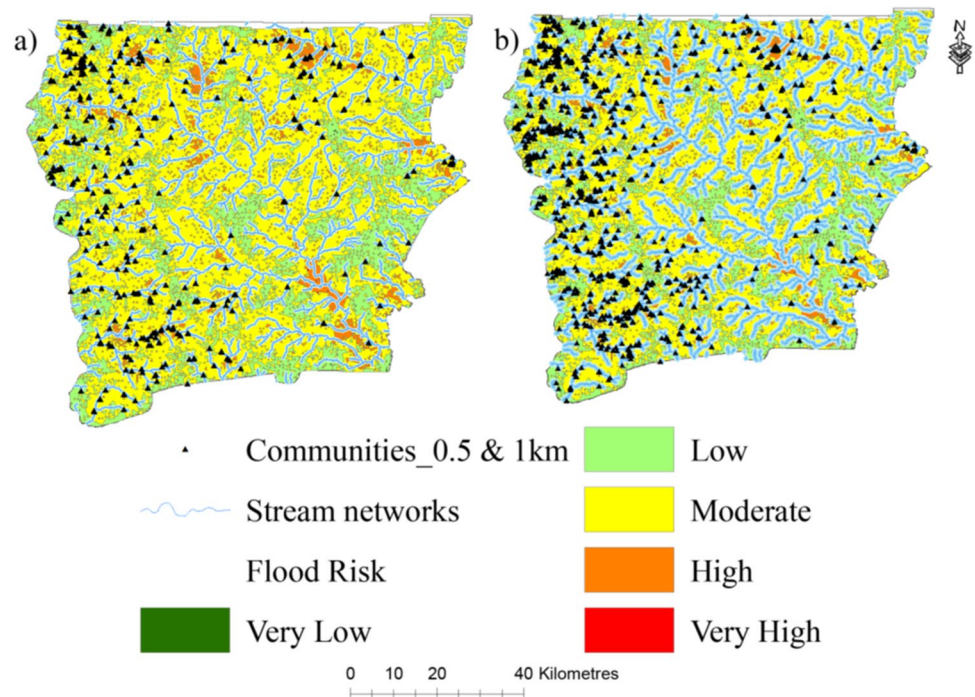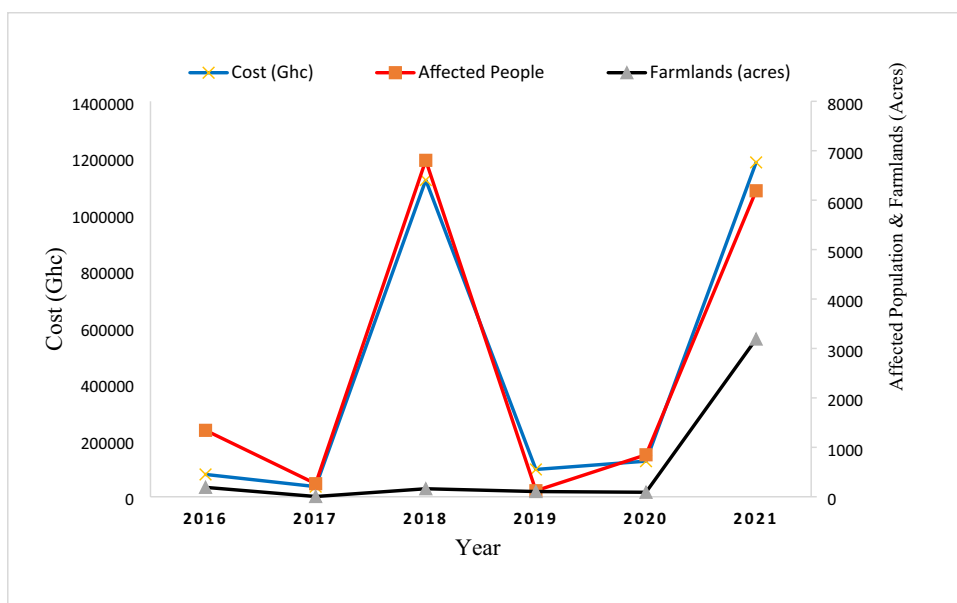
Fig. 8 Cost (Ghs), affected population, and farmlands (Acres)

was higher than that in 2021, however, the economic losses cost in 2021 were also higher than in 2018, due to the massive destruction of many infrastructure; such as roads and culverts, crops, and houses/homes. The poorer settlers in vulnerable areas are largely affected due to their inability to afford safer places and arable lands for agricultural activities within the rural communities (Singer 2018).

This therefore showed, that population growth rate is also a key influencer of flood occurrences as human activities; agriculture, infrastructure, businesses, roads and settlements encroach on natural waterways, low-lying areas, wetlands, valleys, runoff retention/detection areas and increased impervious areas, and reduce the natural drainage systems (Singer 2018; Kaiser et al. 2021; Pham et al. 2021; Gaisie and Cobbinah 2023). The number of crop acres destroyed in 2021 (Fig. 8) is the confirmation of agricultural activities sandwiching wetlands, waterways, low elevations, valleys, and rivers/streams. Most especially, rice farming is the most predominant in those areas. The population of the UWR has steadily increased from 702,110 in 2010 to 901,502 in 2021, indicating a growth rate of 28.40% per year (Fig. 9b). This growth is likely to continue in the future, as the region is experiencing a significant influx of people due to factors such as rural–urban migration, high birth rates, establishment of new educational faculties and improved healthcare, as well as economic activities. Therefore, analysing the population trends in the region is an indispensable aspect of future flood hazards/risks assessment and sustainable management. Figure 9a, b, and c), shows that the population in the region and the districts has been increasing over the 10 years (2010–2021). Nevertheless, the population data was estimated between 2012 and 2020 except for 2021 data,

where population data was recorded through the National Population and Housing Census (PHC) project (GSS 2021).

Statistically, there has been about a 28.40 per cent population increase between 2010 and 2021.

$$Rate\ of\ Change = \frac{901502 - 702110}{702110} \times 100$$
$$= 28.39896882\% \sim 28.40\%.$$

Observations from Fig. 9c, also revealed that districts; Jirapa, Lawra, Lambussie Karni, and Nandom saw a drop in population growth, along with Daffiama Bussie Issa (DBI), which also experienced a little drop in its populations, according to the figures recorded in 2021. However, other districts maintain a constant increase. Significantly, Wa Municipality, which serves as the regional capital, maintains a consistent increase in population. Population growth is a major contributing factor to flood occurrences of hydrological events (Rahman et al. 2021), particularly in regions and terrains with poor infrastructure and inadequate flood control measures, as well as in this era of climate change (Saksena et al. 2020). Population increases translate into urban sprawl and an increase in human activities encroachment on waterways, low-lying areas, and wetlands (Rahman et al. 2021). In the case of the Upper West Region of Ghana, the following factors may have increased the region's vulnerability to floods, though climate change could play a mastermind too. Figure 8, highlighted a steady increase in population and flood events. These observations further showed that the increase in population decreases the surface runoff retention areas and the natural drainage capacity due to the conversion of natural drainage areas for development projects and encroachment on wetlands as a result of
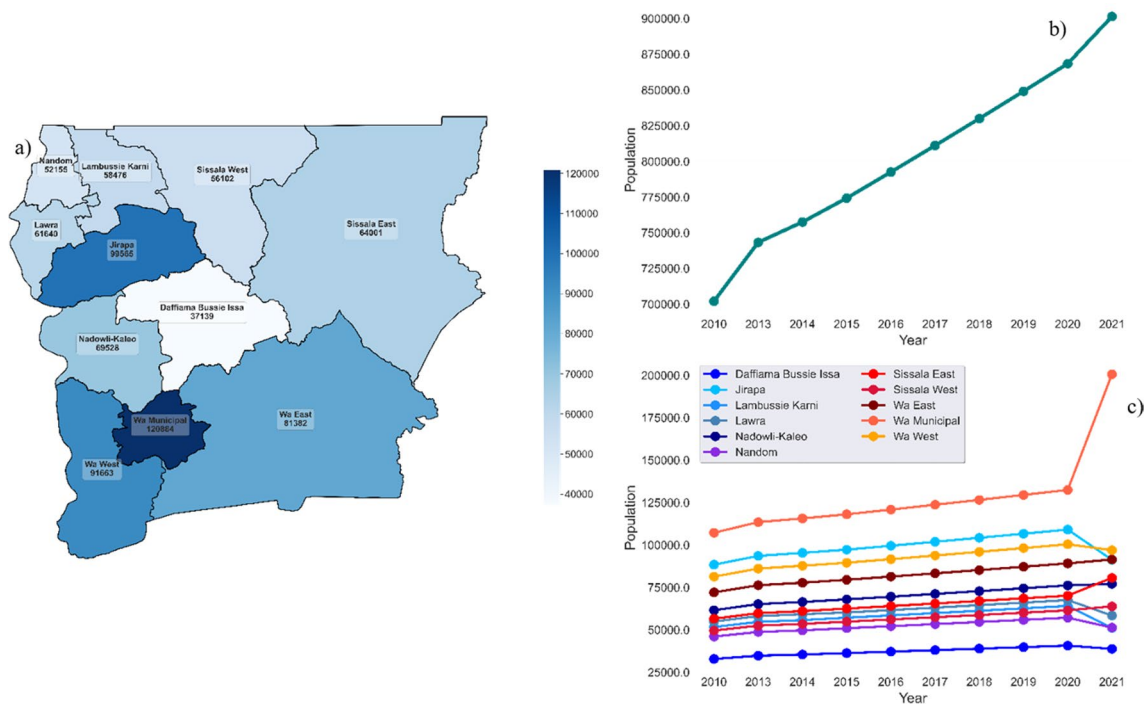
Fig. 9 UWR Population 2010–2021: **a** population map, **b** regional trend, and c Districts' population growth trend

rapid urbanization, these observations were consistent with a study conducted by Seemuangngam and Lin (2024) on the influences of urbanization on urban floods.

Spatial rainfall distributions and floods

Monthly average rainfalls (1992–2022)

Figure 10 presents the spatial distributions of monthly average rainfalls over the 30 years (1992–2022), while Fig. 11 shows the average rainfall for the months of August in each year. The rainfall plot scale ranges approximately around 350 mm/month to below 50 mm/month (Fig. 10). The results (Fig. 10) clearly, revealed that the study area experienced seven (7) months of no or little rainfall. This indicates that October to April serves as the long dry period in the study area as reported by Abu et al. (2024). Arguably, due to the persistent high temperatures that can hit from 40 to 41 degrees Celsius coupled with heatwaves during March and April, rainfalls in April amount to little to nothing before the commences of the rainy season in May (Dery et al. 2023; Abu et al. 2024). The spatial distribution clearly showed an indication that the dry season intensely lasts between November and March as the rains completely recede in October. The observations further illustrated that the rainy seasons in the UWR are between May and September. Additionally, the results highlighted that the rainfall peaks from June to September (JJAS) with exhibitions

of non-homogeneity (Fig. 10), these observations were consistent with the study area's climatic conditions (Dery et al. 2023; Abu et al. 2024). However, the month of August exhibited a strong heterogeneity of rain distribution across the northern part of the region (UWR), largely with the northeastern part of the Sissala West Municipality (SWM) and the northwestern of the Sissala East Municipality (SEM), recording high nucleus of rains magnitude. Consistently, these two municipalities have recorded perennial flood disasters during the rainy season in August. These observations are also in line with the 2007 floods, which were reported to have massively affected populations in both Wa East, Wa West, Sissala East Municipality, and Sissala West Municipality (SWM) (United Nations 2007; Centre Emergency Response Fund 2008). To extensively rule out the fact that the month of August experiences the most perennial floods in the region. Figure 11 also presents the average rainfall results for each August within the 30 years (1992–2022). The total number of months (Augusts) from 1992–2022 analysed was 30 (Fig. 11). The overall mean of the 30 months was computed to be 239.35 mm. The results highlighted some Augusts with higher rainfall depths than others, which is either above or below the overall mean (239.35 mm). The graph showed that, only six (6) Augusts with average rains below 200 mm per month. Illustratively, Augusts in some years; 1996, 2007, 2010, and 2021 also recorded average rainfall peaks over 300 mm. It can be seen from the graph that, the August of 2007 recorded an
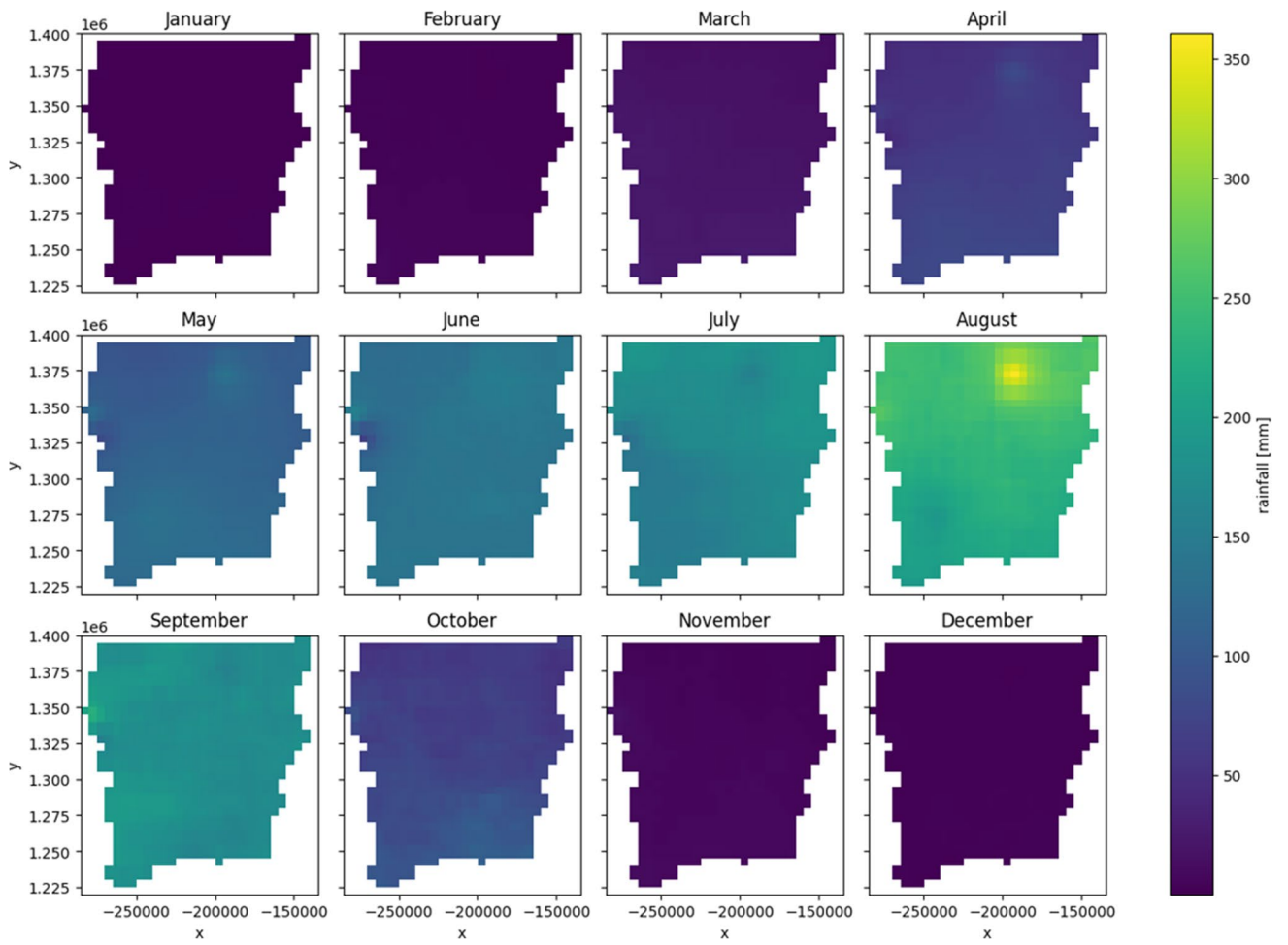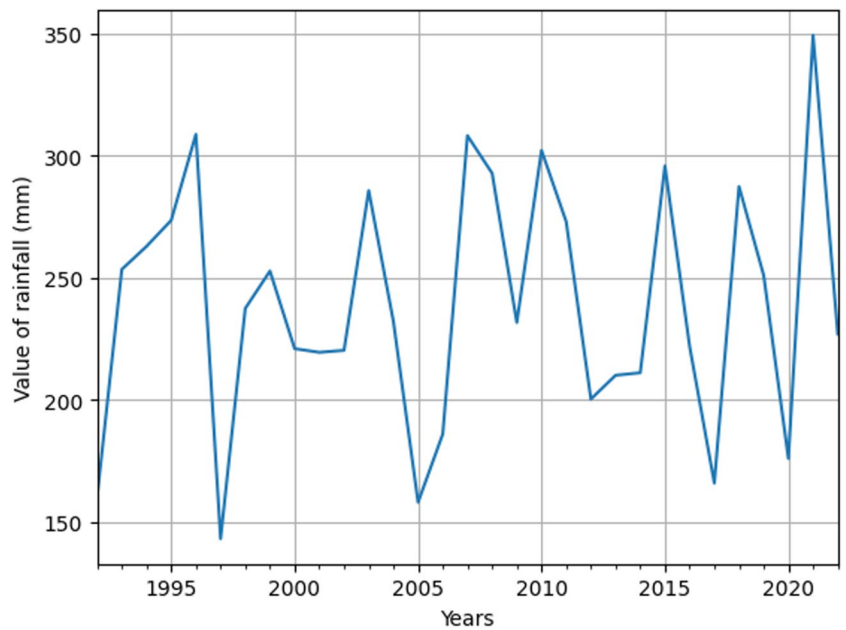
Fig. 10 Spatial distribution of climatology average rainfall (over 30 years) for each month

Fig. 11 Average monthly rainfall for each August: 1992–2022

average rainfall value above 300 mm, where the massive flood disaster occurred in the same August in 2007 (Centre Emergency Response Fund 2008). Significantly, the average rainfall peak amount in August 2021 is approximately 350 mm the highest observed value within the analysis period, this, therefore, confirms why the floods in 2021 were worst of all, after the 2007 flood disaster. All these rainfall findings are consistent with the historical flood disaster records (from 2016–2021) reported in the study area by the NADMO. Additionally, Asumadu-Sarkodie et al. (2015), United Nations (2007), and Centre Emergency Response Fund (2008) reported that the terrible 2007 flood occurred as a result of three (3) weeks of extremely intensive rainfall between August and September 2007. This led to the loss of lives, livestock, properties (homes and schools), foodstuff, water supply systems and roads were also destroyed. The government in 2007 pronounced the study area and other regions (Northern and Upper East regions) as a state of emergency due to the terrible nature of the situations of flood destruction that had occurred. All observations point out August as the most flooding disaster risky month in the study area and generally, the northern parts of the country (IFRC 2023b). This also strengthens the fact that climate change influences droughts and floods through the hydrological cycles (UNESCO 2023a). Further indications from the neighbouring regions (Upper East and Northern) of the country also reported August rains as disastrous. Especially, heavy rainfalls in August of 2018 and 2019 coupled with the perennial spillages of Bagre Dam also caused an unforgettable flood woes in the Upper East region (UER) where Sissala East Municipality and Wa East district share borders (IFRC 2018, 2019). These analyses are consistent with the high nucleus of rainfall magnitude in the Sissala East Municipality and the Sissala West Municipality (SWM) (Fig. 10) and the Augusts average rainfall (Fig. 11). Subsequently, rainfalls forecast on May 5, 2023, by the Ghana Meteorological Agency (GMet) reported, heavy rainfall peaks above normal depths in the UER, while observations in the Upper West, Savannah, North and North East regions ranged from normal to above normal depths till early weeks of September (IFRC 2023b). The current findings affirm the manifestation of flooding during period of heavy rainfalls in the study (Centre Emergency Response Fund 2008; Owusu et al. 2017; IFRC 2018, 2019, 2023b; IPCC 2022). It is also noted at the recede of the 2022 rainy season (GMet 2022), FAO (2022) reported over 80 k hectares of crops had been washed off by floods under influence of heavy rainfalls between August and October 2022 in the northern parts of the country with the study area inclusive.

The findings further reflect the shreds of evidence of heavy and intensive rainfall contributions to flood disasters, which has been widely reported around the globe (Das 2019; Anwana and Owojori 2023; Ncube et al. 2023; Pandey

et al. 2023; Plataridis and Mallios 2023). West Africa subregion alone has over the past decades recorded several flood occurrences during the rainy seasons (Ntajal et al. 2017; Miller et al. 2022). Flooding has been projected to worsen as climate changes through its propelling conditions of extreme rainfalls (IPCC 2022). To buttress the synergy of rainfalls and flooding, the IPCC (2023a, b) further reported an increasing correlation between rains and floods. The findings demonstrated a trend of the relation of how rains in the study area keep nurturing floods in the vulnerable villages, communities, districts and municipalities in the region.

Spatial patterns of average rainfall distributions

Figure 12, also presents the variations of the spatial distribution of annual average rainfall patterns over 30 years (1992–2022); ranging on a scale from 60 mm/yr to 110 mm/yr. From Fig. 12, the presentation highlights the low and high magnitude rainy areas distributed over the study area. The least rainy years were observed to be 1992, 2005, 2013, and 2017 in the study area (Fig. 12). The northwestern and middle parts of the region experienced the least amount of rain in 1992 and 2005 respectively. The southern part of the region also experienced the least distribution of rainfall in 2013 and 2017. The findings further revealed that the northeastern parts; both the Sissala East Municipality (SEM) and Sissala West Municipality (SWM) experienced a high depth of rainfall in 1994. Significant rainfalls were observed to have partly distributed over the region in 2003, 2006, 2010, and 2012. Additionally, a high magnitude of rains was also noted over the region in 1999, with much being felt in both the Sissala East Municipality (SEM) and Sissala West Municipality (SWM). The results revealed strong spatiotemporal observations throughout the region in 2018 and 2019, though more observations were seen along the SEM and SWM, and the Wa East. Significantly, the high rainy trends were observed in 1999, 2018, 2019, and 2021 within the scale of 90 – 100 mm/yr. This further showed that the seasonal rain trends during the 30 years have been not homogeneously distributed over the study area (UWR). These presentations highlighted the rainfall dynamics information over the region, providing a spatiotemporal pattern of the rainfall behaviour in the municipalities and districts. Furthermore, these presentations aligned with the understanding that rainfall trends are influenced by climate change dynamics, that affect the presence of water, and the strengthening of floods and droughts (Wani et al. 2017). The heavy rainy seasons are the key factors inciting floods, and due to the inability of rivers, streams, channels, and low-lying areas to discharge a high volume of surface runoff flows, results in inundations of their catchments and or riparian communities (Nahin et al. 2023). The findings were observed to be consistent with the historical flood events reported by the
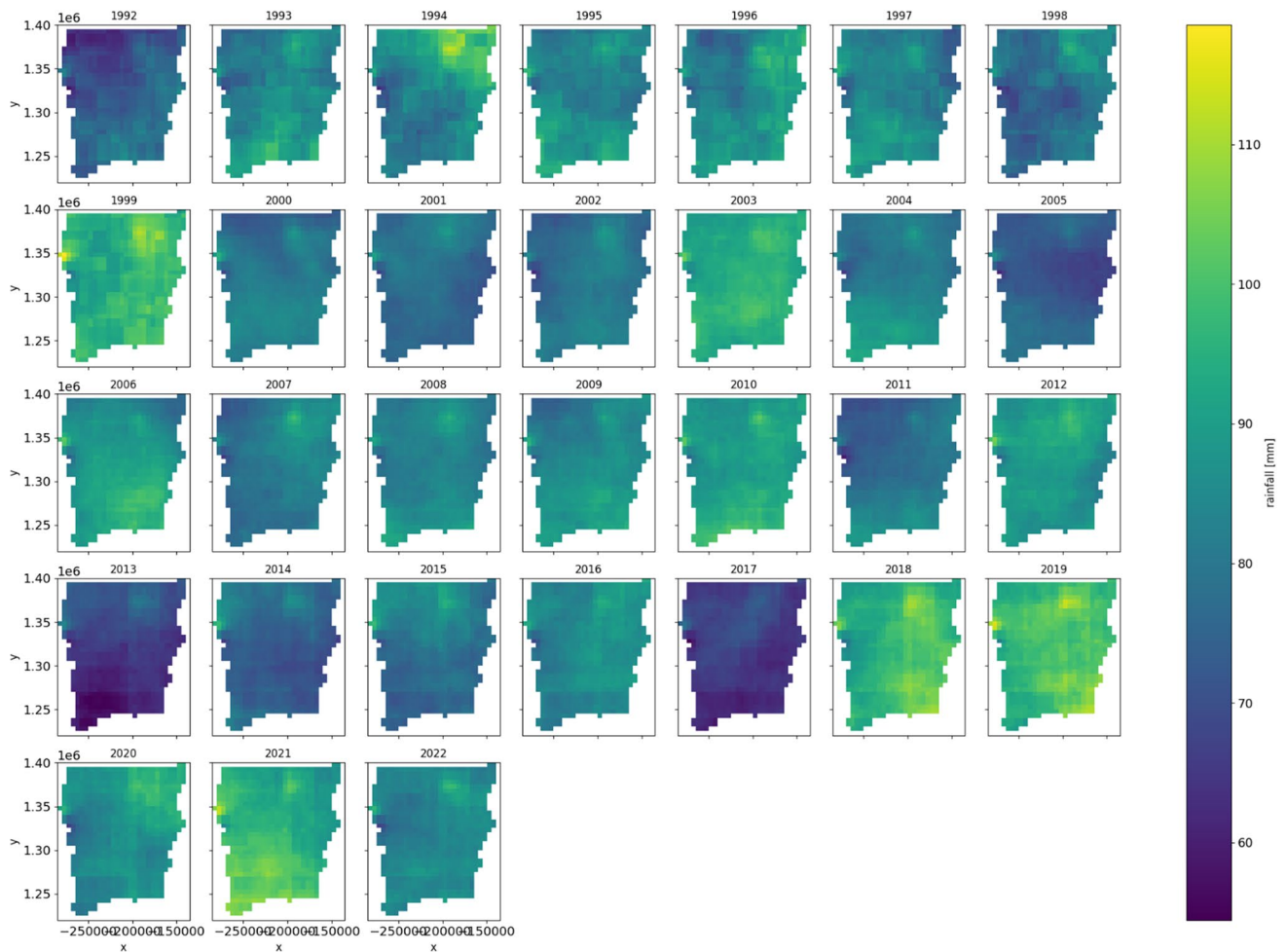
Fig. 12 Spatial distribution of annual average rainfall (mm/yr)

NADMO in the study area. Additionally, the high spatial distribution of rainfalls, largely in the 2016, 2018, 2020, and 2021 affirms flood disasters reported.

Figure 13 represents 5 years categorization of spatial annual average rainfall distribution (1993–2022). From the analysis, both Figs. 12 and 13 visualizations show distinctive similarities of heightened rainfalls along the eastern SWM and northwestern SEM. The NADMO has so far identified several communities as flood prone communities, with 9 and 15 communities in the SWM and SEM, respectively. Notably, from the 1990s to 2022, parts of the study area experienced a series of perennial flood events that were largely attributed to the severity and the intensive nature of rainfalls during the rainy seasons. Perennial flood manifestation between 2016 and 2022, in the study area has been under an upward rise in flooding events, particularly linked to the spatial distribution of the rains in the region. As illustrated in Fig. 13, the highlights revealed that a less substantial amount of rain (75–85 mm/5yrs) was observed within the middle and southern parts of the region in 2017–2022. On the contrary, the historical flood events

documented show destructions of flood episodes all over the middle belt and the southern parts. This is a confirmation of fewer rains resulting in flood perennial floods mostly during seasons. As global climatic patterns have disrupted the ecological system of the study area, extreme rainfalls in the rainy seasons become intensive, manifesting severe natural disasters; floods and longer droughts in the dry seasons. This has underscored the need for sustainable mitigation measures to address flooding and drought impacts in vulnerable communities within intensive rainy zones. Unforgettable, in August 2021, the study area experienced unusual rainfall between the 12th and 13th of August, which resulted in devasting flooding, that swept away farms and homes, and disrupted roads, with almost all the districts and municipalities being blocked from the regional capital. The national road linking Ghana and Burkina Faso through the region was also massively cut off, as several culverts were swept away. This signified the severity and intensity of the rainfall within two days that led to the terrible flood disaster. The spatial highlights of the visual rainfall distributions (Fig. 13), provide critical insightful information
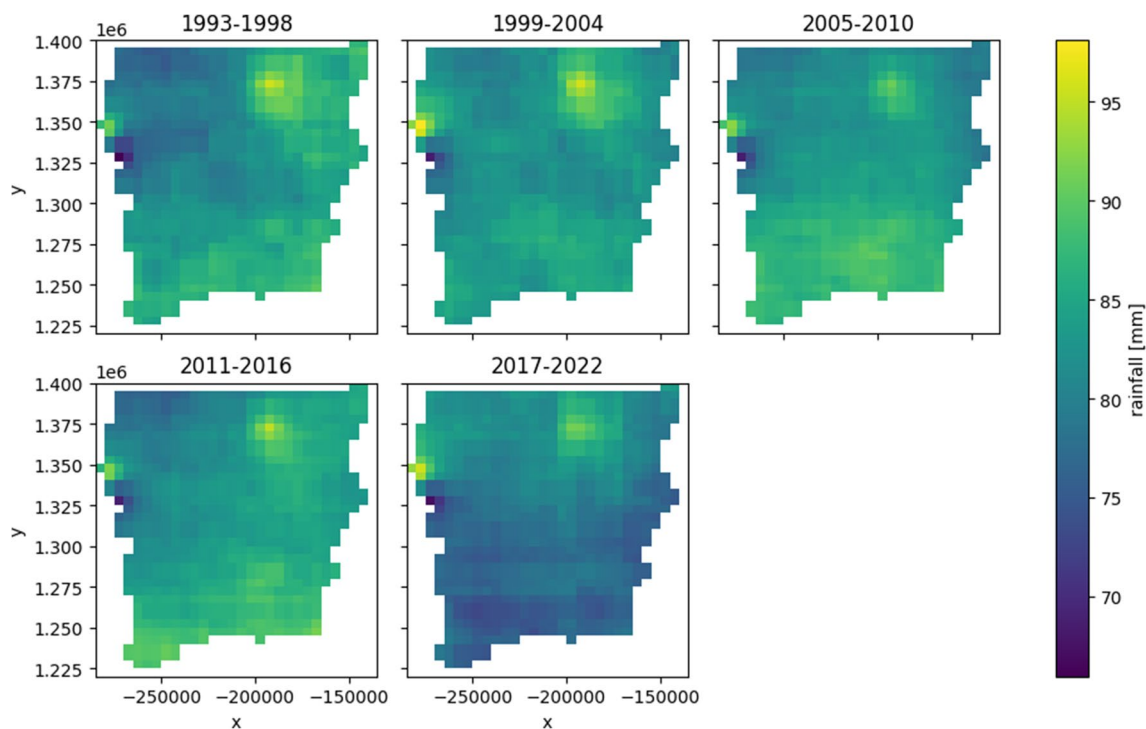
Fig. 13 Spatial patterns of rainfall distribution (1993–2022): Five (5) year annual average(mm/5yrs)

on the amount and patterns of rainfalls experienced over the study area during the period of the analysis.

As delineated in Fig. 13, the communities that felt within the heavy rainy areas (80 to 95 > mm/5yrs) were exposed to the consequences of multiple flood episodes. This therefore affirms that when the rivers and streams become incapacitated of channelling out a high volume of rainwater results in floods in the communities (Nahin et al. 2023). This further strengthens the fact that rainfall is one of the key causes of flood disasters in the Upper West region. Though the intensity of rainfalls alone cannot qualify it as the main cause of flood disasters (Garba and Abdourahamane 2023), however, several flood disasters over the years within the region and country, and around the globe have been linked to heavy rainfalls (Paeth et al. 2011; Okyere et al. 2013; Asumadu-Sarkodie et al. 2015; Kwang and Osei Jnr 2017; Cabrera and Lee 2019; Sacré Regis et al. 2020; Osei et al. 2021a, b; Alifu et al. 2022; Danso et al. 2024; Nagamani et al. 2024; Rączkowska et al. 2024). It has also been noted that heavy rains as an extreme weather event often result in natural hazards with floods alike (World Economic Forum 2024).

Correlation matrix of historical rainfalls and flood disasters

The correlation matrix (Fig. 14) was also used to measure the magnitude of August's heavy rainfalls and their association with historical flood events. Therefore, the average Augusts rainfalls (2016–2022), and the six years of historical flood records available data (affected population, farmlands, and cost of disasters) were used as the elements of proportionality to compute the correlation matrix to confirm the Augusts rainfalls relationship with floods, that have a strong association on elements within the study area. The correlation matrix is based on a scale range of $-1 \leq r \leq +1$, where r could represent -1, 0, and + 1, as a negative proportionality of each two elements, no correlation/non-association, and proportionality of each two elements respectively (Castleman and Wu 2023). Schober and Schwarte, (2018) indicated that a strong correlation is from 0.7 to 0.89, a very strong correlation ranges from 0.99 to 1.0, while a moredate correlation also ranges from 0.40 to 0.69. The results (Fig. 14) showed a strong correlation of the rainfalls with the affected population, farmlands (acres), and cost (Ghc) with r values of 0.82, 0.78 and 0.87, respectively. The economic losses (Cost (Ghc)) and the affected population exhibited a very strong correlation of 0.99, while farmlands (acres) and the affected population recorded a moderate correlation of 0.6. However, the cost (Ghc) and farmlands (acres) also reported a moderate correlation with an $r \leq 0.67$. These analyses further strengthen the relationship between rainfalls and flood events' effects on citizens and the general ecosystem.

Fig. 14 Paired correlation of rainfall and flood effects
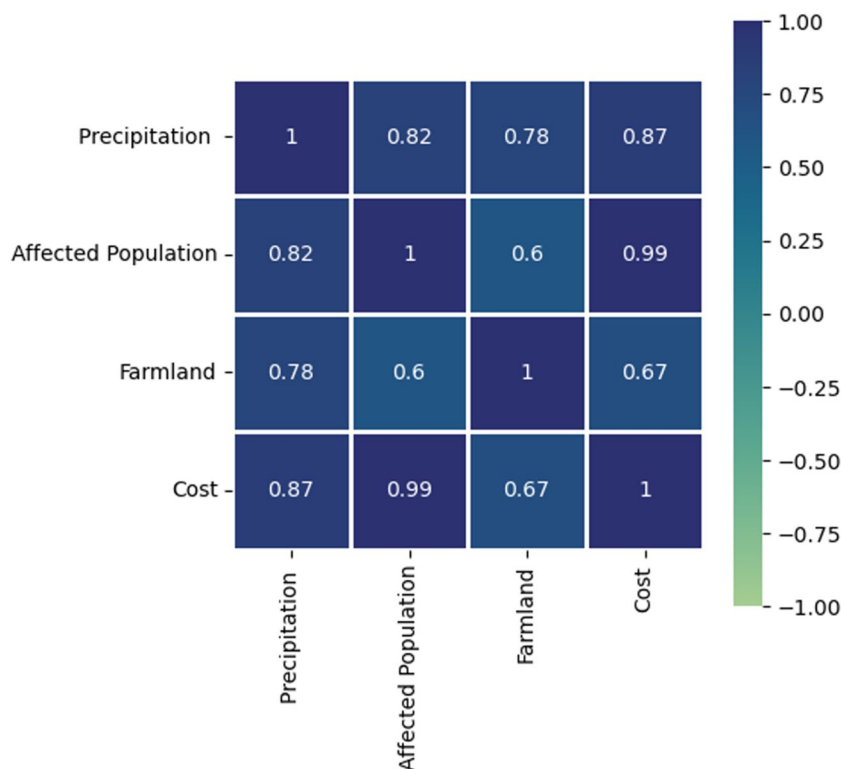
Conclusion and recommendations

The main goals of this study are to delineate flood risk terrains, buffer zoning of communities along rivers/streams, evaluate historical flood records and population trends, and visualization of rainfall behaviour, which are proactive measures for the management and mitigation of perennial floods in the Upper West Region. The study primarily proceeded with Jenks natural breaks classification (JNBC) (Jenks 1967) technique and GIS-based Analytical Hierarchy Process (AHP) multi-criteria decision (AHP-MCD). JNBC technique employed only SRTM DEM to first optimize the areas likely to be susceptible to flood. The GIS-based AHP multi-criteria decision algorithm also incorporated six geospatial flood conditioning factors comprising Lineament Density, Elevation, Topographic Wetness Index, Drainage Density, Slope, and Aspect. This was done based on literature and the availability of datasets. Buffer zones of 0.5 km and 1 km were also created around the streams/river networks to determine the number of communities that will be inundated during fluvial floods. The outcomes of JNBC algorithm reclassification indicate that the UWR can be categorized into five classes; very high risk to very low risk terrains covering 4% (856.278 km^2), 7% (1466.685 km^2), 12% (2418.642 km^2), 35% (7014.96 km^2), and 42% (8351.496 km^2), respectively. The performance of the JNBC flood risk terrains map generated was evaluated with ground truthing points (GTPs) of 85 historical flood points, this was done by

overlaying the GTPs on the map, while computing the number of GTPs on each class of the map as a percentage. The very low flood risk terrains recorded 31.76% of the GTPs while the very high flood risk terrains recorded the lowest GTPs with 11.76%.

The AHP-MCD integration of the six sub-thematic flood conditioning factors also characterized the total study area into five classes; very high, high, medium, low, and very low with coverages as 0.707 km^2 (0.004%), 3830.02 km^2 (21%), 12,807.31 km^2 (69%), 1827.011 km^2 (10%), and 11.535 km^2 (0.062%), respectively. During the validation, the moderate flood risk terrains class attained 71.76% of the GTPs as compared with the other classes, thus signifying that the classes generated were accurate for decision-making in the study area, and largely indicated the study falls within moderate flood risk terrains.

The spatial outlines of the very high flood risk terrains and high flood risk terrains classes of both the JNBC and AHP-MCD maps are situated along the southeastern and eastern fringes of the study area, that is, Sissala East Municipality (SEM) and Wa East district (WED), and primarily sited along the major river networks, agreeing that low-lying areas are more susceptible to flood disasters in the study area.

The agreement of the GTPs (historical flood points) and the flood risk terrains generated by the AHP-MCD method, improved the acceptance of the results for flood policy formulation and communication, sustainable flood

mitigation strategies and management, and as well as the public perception of flood disasters (Houston et al. 2019).

From the selected buffer ranges; 0.5 km and 1 km, communities sandwiched between the buffered ranges were classified as vulnerable to flooding as compared to those outside the ranges, during an overflow of the rivers and streams.

The spatial visualization of the rainfall patterns distribution highlights the important role rainfalls play in flood assessment. The CHIRPS data analysed revealed the distribution of the heightened rainfall over flood risk terrain communities. The historical flooding records over the years, months and communities were consistent with the spatial rainfall distributions especially the month of August.

This study contributes valuable insights into spatial flood and extreme rainfall patterns distribution in the study area.

It emphasizes that the town and country planning, municipalities and district assemblies ensure that buffer zoning rules are strictly enshrined in community, town, and city planning, and the allocation of areas for broad farming.

Farmers need to plant short maturity period seeds and crops that can be harvested before floods commence or that stay in flood waters for a period. Most especially rice and maize cropping in the region, though rice is a hydrophobic crop, however, the flood water resistant variety should be encouraged in the region, mostly for those farming along the risky areas.

The findings underscore, further studies using machine learning algorithms to analyse satellite imagery data for inundation through the integration of advanced scientific hydroclimatic modelling and simulations and stakeholder engagement around the communities to prepare resilient proactive measures to tackle future flood events.

Declarations

Ethical approval Not applicable.

Consent to participate Agree to participate.

Consent to publish Agree to publish.

Conflict of interest The authors declare no conflicts of interest.

References

Abdrabo KI, Kantoush SA, Esmaiel A, Saber M, Sumi T, Almamari M, Elboshy B, Ghoniem S et al (2023) An integrated indicator-based approach for constructing an urban flood vulnerability index as an urban decision-making tool using the PCA and AHP techniques: a case study of Alexandria, Egypt. Urban Clim 48:1–19. https://doi.org/10.1016/j.uclim.2023.101426

Abdul-ganiyu S, Kpiebaya P (2020) Groundwater resources as a resilient alternative for irrigation in the Upper West Region of Ghana – a study of groundwater potential. Int J Innov Sci Res Tech 5:1–10

Abu M, Zango MS, Kazapoe R (2024) Controls of groundwater mineralization assessment in a mining catchment in the Upper West Region, Ghana: Insights from hydrochemistry, pollution indices of groundwater, and multivariate statistics. Innov Green Dev 3:1–14. https://doi.org/10.1016/j.igd.2023.100099

Addis A (2022) GIS – based flood susceptibility mapping using frequency ratio and information value models in Upper Abay River Basin, Ethiopia. SSRN Electron J 3:247–256. https://doi.org/10.2139/ssrn.4246701

Adel S, Fazel A, Mirfenderesk H, Tomlinson R, Blumenstein M (2014) Estuarine flood modelling using artificial neural networks Estuarine flood modelling using Artificial Neural Networks. in 2014 International Joint Conference on Neural Networks (IJCNN). IEEE, Beijing, China pp 631–637. https://doi.org/10.1109/IJCNN.2014.6889704

Aerts JCJH, Botzen WJ, Clarke KC, Cutter SL, Hall JW, Merz B, Michel-Kerjan E, Mysiak J, Surminski S, Kunreuther H (2018) Integrating human behaviour dynamics into flood disaster risk assessment. Nat Clim Change 8:193–199. https://doi.org/10.1038/s41558-018-0085-1

Ahadzie DK, Mensah H, Simpeh E (2021) Impact of floods recovery and repairs of residential structures in Ghana: insights from homeowners. GeoJournal 87:3133–3148. https://doi.org/10.1007/s10708-021-10425-2

Ahmad I (2018) Digital elevation model (DEM) coupled with geographic information system (GIS): an approach towards erosion modeling of Gumara watershed Ethiopia. Environ Mon Assess 190:1–18. https://doi.org/10.1007/s10661-018-6888-8

Ahmed I, Das (Pan) N, Debnath J, Bhowmik M, Bhattacharjee S (2024) Flood hazard zonation using GIS-based multi-parametric analytical hierarchy process. Geosyst Geoenviron 3(2). https://doi.org/10.1016/j.geogeo.2023.100250

Al-Areeq AM, Sharif HO, Abba SI, Chowdhury S, Al-suwaiyan M, Benaafi M, Yassin MA, Aljundi IH (2023) International journal of applied earth observation and geoinformation digital elevation model for flood hazards analysis in complex terrain: case study from Jeddah Saudi Arabia. Int J Appl Earth Observ Geoinform 119:1–13. https://doi.org/10.1016/j.jag.2023.103330

Al-Taani A, Al-husban Y, Ayan A (2023) Assessment of potential flash flood hazards. Concerning land use/land cover in Aqaba Governorate Jordan using a multi-criteria technique. Egypt J Remote Sens Space Sci 26:17–24. https://doi.org/10.1016/j.ejrs.2022.12.007

Alifu H, Hirabayashi Y, Imada Y, Shiogama H (2022) Enhancement of river flooding due to global warming. Sci Rep 12:20687. https://doi.org/10.1038/s41598-022-25182-6

Alimi SA, Andongma TW, Ogungbade O, Senbore SS, Alepa VC, Akinlabi OJ, Olawale LO, Muhammed QO (2022) Flood vulnerable zones mapping using geospatial techniques: case study of Osogbo Metropolis, Nigeria. Egypt J Remote Sens Space Sci 25:841–850. https://doi.org/10.1016/j.ejrs.2022.08.003

Amen ARM, Mustafa A, Kareem DA, Hameed HM, Mirza AA, Szydłowski M, Saleem BKM, (2023) Mapping of flood-prone

areas utilizing GIS techniques and remote sensing : mapping of flood-prone areas utilizing GIS techniques and remote sensing : a case study of Duhok Kurdistan Region of Iraq. Remote Sens 15. https://doi.org/10.3390/rs15041102

Amirruddin AD, Muharam FM, Ismail MH, Ismail MF, Tan NP, Karam DS (2020) Hyperspectral remote sensing for assessment of chlorophyll sufficiency levels in mature oil palm (Elaeis guineensis) based on frond numbers: analysis of decision tree and random forest. Comput Electron Agric 169:1–11. https://doi.org/10.1016/j.compag.2020.105221

Amoako C, Boamah EF (2014) The three-dimensional causes of flooding in Accra, Ghana. Intl J Urban Sustain Develop 7(1):109–129. https://doi.org/10.1080/19463138.2014.984720

Anchang JY, Ananga EO, Pu R (2016) An efficient unsupervised index based approach for mapping urban vegetation from IKONOS imagery. Int J Appl Earth Obs Geoinf 50:211–220. https://doi.org/10.1016/j.jag.2016.04.001

Asumadu-Sarkodie S, Owusu PA, Rufangura P (2015) Impact analysis of flood in Accra Ghana. Adv Appl Sci Res 6:53–78. https://doi.org/10.6084/M9.FIGSHARE.3381460

Andrade L, O'Dwyer J, O'Neill E, Hynds P (2018) Surface water flooding groundwater contamination and enteric disease in developed countries: a scoping review of connections and consequences. Environ Pollut 236:540–549. https://doi.org/10.1016/j.envpol.2018.01.104

Andualem TG, Demeke GG (2019) Groundwater potential assessment using GIS and remote sensing: a case study of Guna tana landscape upper blue Nile Basin Ethiopia. J Hydrol: Reg Stud 24:1–13. https://doi.org/10.1016/j.ejrh.2019.100610

Anwana EO, Owojori O (2023) Literature : mapping and research agenda. Soc Sci Rev 12:1–21

Arabameri A, Rezaei K, Pourghasemi HR et al (2018) GIS-based gully erosion susceptibility mapping: a comparison among three data-driven models and AHP knowledge-based technique. Environ Earth Sci 77:628. https://doi.org/10.1007/s12665-018-7808-5

Arabameri A, Saha S, Chen W, Roy J, Pradhan B, Bui DT (2020) Flash flood susceptibility modelling using functional tree and hybrid ensemble techniques. J Hydrol 587:125007. https://doi.org/10.1016/j.jhydrol.2020.125007

Armah FA, Yawson DO, Yengoh GT, Odoi JO, Afrifa EKA (2010) Impact of floods on livelihoods and vulnerability of natural resource dependent communities in Northern Ghana. Water 2:120–139. https://doi.org/10.3390/w2020120

Association of State Floodplain Managers (2020) Flood mapping for the nation: a cost analysis for completing and maintaining the Nation's NFIP flood map inventory. Available at: https://asfpm-library.s3-us-west-2.amazonaws.com/FSC/MapNation/ASFPM_MaptheNation_Report_2020.pdf. Accessed 8 May 2024

Atiah WA, Amekudzi LK, Aryee JNA, Preko K, Danuor S (2020) Validation of satellite and merged rainfall data over Ghana West Africa. Atmosphere 11:1–23. https://doi.org/10.3390/ATMOS11080859

El Ayady H, Mickus KL, Boutaleb S, El Morjani ZEA, Ikirri M, Echogdali FZ, Ekoa Bessa AZE, Abdelrahman K, Id-Belqas M, Essoussi S, Fnais MS, Abioui M (2023) Investigation of groundwater potential using geomatics and geophysical methods: case study of the Anzi sub-basin western Anti-Atlas Morocco. Adv Space Res 72:3960–3981. https://doi.org/10.1016/j.asr.2023.08.044

Ayehu GT, Tadesse T, Gessesse B, Dinku T (2018) Validation of new satellite rainfall products over the Upper Blue Nile Basin Ethiopia. Atmos Meas Tech 11:1921–1936. https://doi.org/10.5194/amt-11-1921-2018

Ayenew WA, Kebede HA (2023) GIS and remote sensing based flood risk assessment and mapping: the case of Dikala Watershed in Kobo Woreda Amhara Region Ethiopia. Environ Sustain Indic 18:100243. https://doi.org/10.1016/j.indic.2023.100243

Aznar-crespo P, Aledo A, Melgarejo-moreno J, Valllejos-Romero A (2021) Adapting social impact assessment to flood risk management. Sustainability 13:1–27. https://doi.org/10.3390/su13063410

Baci NO, Jafarzadegan K, Moradkhani H (2024) Improving flood inundation modeling skill: interconnection between model parameters and boundary conditions. Model Earth Syst Environ 10:243–257. https://doi.org/10.1007/s40808-023-01768-5

Baddianaah I, Baatuuwie BN, Adongo R (2022) Geospatial characterisation and distribution of Illegal gold mining (galamsey) operations in Upper West Region Ghana. GeoJournal 88:789–810. https://doi.org/10.1007/s10708-022-10642-3

Ball J (2011) Soil and water relationships. Ag News and Views 1–3. Available at: https://kbsgk12project.kbs.msu.edu/wp-content/uploads/2011/09/Soil-and-Water-Relationships.pdf. Accessed 9 Sept 2021

Bello IE, Ogedegbe SO (2015) Geospatial analysis of flood problems in Jimeta riverine community of Adamawa State Nigeria. J Environ Earth Sci 5:32–45. Available at: http://www.iiste.org/Journals/index.php/JEES/article/view/23299/24045. Accessed 19 Oct 2023

Brulard N (2011) Agrarian system diagnosis around Wa upper west region Ghana

Bullen J, Miles A (2024) Exploring local perspectives on flood risk: a participatory GIS approach for bridging the gap between modelled and perceived flood risk zones. Appl Geogr 163:1–10. https://doi.org/10.1016/j.apgeog.2023.103176

Cabrera JS, Lee H (2019) Flood-prone area assessment using GIS-based multi-criteria analysis: a case study in Davao Oriental Philippines. Water (Switzerland) 11:1–23. https://doi.org/10.3390/w11112203

Castleman KR, Wu Q (2023) Object classification. in microscope image processing second edition. Elsevier Inc, pp 177–200. https://doi.org/10.1016/B978-0-12-821049-9.00010-1

Centre Emergency Response Fund (2008) Annual report of the humanitarian/resident coordinator on the use of CERF Grants. Available at: https://cerf.un.org/sites/default/files/resources/CERF%202007%20Annual%20Report%20DPRK%20FINAL_WEB.pdf. Accessed 8 May 2024

Centre for Research on the Epidemiology of Disasters (2018) Flash floods sharing of field experience-Kerala. Cred Crunch 53:1–2

Centre for Research on the Epidemiology of Disasters (2019) Disasters in Africa: 20 year review 2000–2019 (issue 56, 1–2). In: Centre for Research on the epidemiology of disasters. Available at: https://www.cred.be/sites/default/files/CredCrunch56.pdf. Accessed 10 Feb 2024

Centre for Research on the Epidemiology of Disasters (2023) 2022 disasters in numbers. CRED, Brussels. Available at: https://cred.be/sites/default/files/2022_EMDAT_report.pdf. Accessed 6 Apr 2023

Chowdhuri I, Pal SC, Chakraborty R (2020) Flood susceptibility mapping by ensemble evidential belief function and binomial logistic regression model on river basin of eastern India. Adv Space Res 6:1466–1489. https://doi.org/10.1016/j.asr.2019.12.003

Costache R, Arabameri A, Blaschke T, Pham QB, Pham BT, Pandey M, Arora A, Linh NTT, Costache I (2021) Flash-flood potential mapping using deep learning alternating decision trees and data provided by remote sensing sensors. Sensors (Switzerland) 21:1–21. https://doi.org/10.3390/s21010280

Costache R (2019) Flash-flood potential index mapping using weights of evidence decision trees models and their novel hybrid integration. Stoch Env Res Risk Assess 33:1375–1402. https://doi.org/10.1007/s00477-019-01689-9

Danso SY, Ma Y, Osman A, Addo IY (2024) Integrating multi-criteria analysis and geospatial applications for mapping flood hazards in Sekondi-Takoradi Metropolis, Ghana. J African Earth Sci 209. https://doi.org/10.1016/j.jafrearsci.2023.105102

Danumah JH, Odai SN, Saley BM, Szarzynski J, Thiel M, Kwaku A, Kouame FK, Akpa LY (2016) Flood risk assessment and mapping in Abidjan district using multi-criteria analysis (AHP) model and geoinformation techniques (Cote d'Ivoire). Geoenviron Disasters 3:1–13. https://doi.org/10.1186/s40677-016-0044-y

Das S, Pardeshi SD (2017) Comparative analysis of lineaments extracted from Cartosat SRTM and ASTER DEM: a study based on four watersheds in Konkan region India. Spat Inform Res 26:47–57. https://doi.org/10.1007/s41324-017-0155-x

Das S (2017) Delineation of groundwater potential zone in hard rock terrain in Gangajalghati block, Bankura district, India using remote sensing and GIS techniques. Model Earth Syst Environ 3:1589–1599. https://doi.org/10.1007/s40808-017-0396-7

Das S (2019) Geospatial mapping of flood susceptibility and hydro-geomorphic response to the floods in Ulhas basin India. Remote Sens Appl: Soc Environ 14:60–74. https://doi.org/10.1016/j.rsase.2019.02.006

Dazzi S, Vacondio R, Mignosa P (2021) Flood stage forecasting using machine-learning methods : a case study on the Parma River (Italy). Water 13:1612. https://doi.org/10.3390/w13121612

Debnath J, Sahariah D, Nath N et al (2024) Modelling on assessment of flood risk susceptibility at the Jia Bharali River basin in Eastern Himalayas by integrating multicollinearity tests and geospatial techniques. Model Earth Syst Environ 10:2393–2419. https://doi.org/10.1007/s40808-023-01912-1

Dekongmen BW, Kabo-bah AT, Domfeh MK, Sunkari ED et al (2021) Flood vulnerability assessment in the Accra Metropolis, southeastern Ghana. Appl Water Sci 11(7):1–10. https://doi.org/10.1007/s13201-021-01463-9

Deroliya P, Ghosh M, Mohanty MP, Ghosh S, Rao KHVD, Karmakar S (2022) A novel flood risk mapping approach with machine learning considering geomorphic and socio-economic vulnerability dimensions. Sci Total Environ 851:1–14. https://doi.org/10.1016/j.scitotenv.2022.158002

Dery BP, Sanyare FN, Gyader GN (2023) Achieving greater participation in agricultural production: A study of government workers in the Upper west region of Ghana. Heliyon 9:1–14. https://doi.org/10.1016/j.heliyon.2023.e21821

Diabene PY, Gyamfi C, Odai SN, Annor FO (2014) Mapping potential areas in the upper west region of Ghana for the implementation of agricultural water management: GIS and remote sensing approach. Int J Dev Sci 3:2059–2076

Dinku T, Funk C, Peterson P, Maidment R, Tadesse T, Gadain H, Ceccato P (2018) Validation of the CHIRPS satellite rainfall estimates over eastern Africa. Q J R Meteorol Soc 144:292–312. https://doi.org/10.1002/qj.3244

Donegan HA, Dodd FJ (1991) A note on Saaty's random indexes. Mathl Comput Modelling 15:135–137. https://doi.org/10.1016/0895-7177(91)90098-R

FAO (2022) "GIEWS country brief Ghana global watch GIEWS". Available at: https://reliefweb.int/report/ghana/giews-country-brief-ghana-28-october-2022. Accessed 28 Oct 2022

Feujio DHA, Aretouyap Z, Tchato SC, Legrand CN, Djomdi E, Madadjeu NN, Nguimgo CN, Kpoumie AN (2024) Application of analytical hierarchy process to assess groundwater potential for a sustainable management in the Menoua Division. Heliyon 10:1–17. https://doi.org/10.1016/j.heliyon.2024.e24310

Fischer S, Schumann AH (2024) Temporal changes in the frequency of flood types and their impact on flood statistics. J Hydro X 22:1–14. https://doi.org/10.1016/j.hydroa.2024.100171

Forson ED, Amponsah PO, Hagan GB, Sapah MS (2023) Frequency ratio-based flood vulnerability modeling over the greater Accra Region of Ghana. Model Earth Syst Environ 9:2081–2100. https://doi.org/10.1007/s40808-022-01616-y

Frimpong A (2014) Perennial floods in the Accra Metropolis: dissecting the causes and possible solutions. Afr Soc Sci Rev 6(1):1. Available at: http://digitalscholarship.bjmlspa.tsu.edu/assr/vol6/iss1/1. Accessed 20 Aug 2021

Funk C, Peterson P, Landsfeld M et al (2015) The climate hazards infrared precipitation with stations—a new environmental record for monitoring extremes. Sci Data 2:1–21. https://doi.org/10.1038/sdata.2015.66

Gacu JG, Monjardin CEF, Senoro DB, Tan FJ (2022) Flood risk assessment using GIS-based analytical hierarchy process in the Municipality of Odiongan Romblon Philippines. Appl Sci 12:1–31. https://doi.org/10.3390/app12199456

Gaisie E, Cobbinah PB (2023) Planning for context-based climate adaptation: Flood management inquiry in Accra. Environ Sci Policy 141:97–108. https://doi.org/10.1016/j.envsci.2023.01.002

Garba I, Abdourahamane ZS (2023) Extreme rainfall characterisation under climate change and rapid population growth in the city of Niamey Niger. Heliyon 9:1–14. https://doi.org/10.1016/j.heliyon.2023.e13326

Garg S, Feinstein B, Timnat S, Batchu V, Dror G, Rosenthal AG, Gulshan V (2023) Cross-modal distillation for flood extent mapping. Environ Data Sci 2:1–19. https://doi.org/10.1017/eds.2023.34

Gaume E et al (2009) A compilation of data on European flash floods. J Hydrol 367:70–78. https://doi.org/10.1016/j.jhydrol.2008.12.028

Getahun YS, Gebre SL (2015) Flood Hazard assessment and mapping of flood inundation area of the Awash River basin in Ethiopia using GIS and HECGeoRAS/HEC-RAS model. J Civil Environ Eng 5:179. https://doi.org/10.4172/2165-784X.1000179

Ghana Statistical Service (GSS) (2013) Regional Analytical Report, Upper West Region. Available at: https://www2.statsghana.gov.gh/docfiles/2010phc/2010_PHC_Regional_Analytical_Reports_Upper_West_Region.pdf. Accessed 27 Aug 2021

Ghana Statistical Service (GSS) (2021) Ghana statistical service 2021 population and housing census press release provisional results. In: Population and housing census: provisional results. Available at: https://statsghana.gov.gh/gssmain/fileUpload/pressrelease/2021%20PHC%20Provisional%20Results%20Press%20Release.pdf. Accessed 28 Jan 2022

Ghosh S, Saha S, Bera B (2022) Flood susceptibility zonation using advanced ensemble machine learning models within Himalayan foreland basin. Nat Hazards Res 2:363–374. https://doi.org/10.1016/j.nhres.2022.06.003

GMet (Ghana Meteorological Agency) (2022) Ghana Meteorological agency's seasonal forecast for the northern sector and seasonal forecast update for the southern sector of Ghana: June-Aug (JJA) and Jul - Sept (JAS) for the country, 2022. Available at: https://www.meteo.gov.gh/gmet/wpcontent/uploads/2022/05/JJA_JAS-Seasonal-Forecast_North-2022.pdf. Accessed 30 Nov 2023

Gómez-Escalonilla V, Martínez-Santos P, Martín-Loeches M (2022) Preprocessing approaches in machine-learning-based groundwater potential mapping: an application to the Koulikoro and Bamako regions Mali. Hydro Earth Syst Sci 26:221–243. https://doi.org/10.5194/hess-26-221-2022

Guoyi L, Liu J, Shao W (2023) Urban flood risk assessment under rapid urbanization in Zhengzhou City China. Reg Sust 4:332–348. https://doi.org/10.1016/j.regsus.2023.08.004

Gupta L, Dixit J (2022) A GIS-based flood risk mapping of Assam India using the MCDA-AHP approach at the regional and administrative level. Geocarto Int 37:11867–11899. https://doi.org/10.1080/10106049.2022.2060329

Houston D, Cheung W, Basolo V, Feldman D, Matthew R, Sanders BF, Karlin B, Schubert JE, Goodrich KA, Contrer S, Luke A (2019) The influence of hazard maps and trust of flood controls

on coastal flood spatial awareness and risk perception. Environ Behav 51:347–375. https://doi.org/10.1177/0013916517748711

Hudson P, Berghäuser L (2023) Investigating moral hazard and property-level flood resilience measures through panel data from Germany. Int J Disaster Risk Reduct 84:103480. https://doi.org/10.1016/j.ijdrr.2022.103480

IFRC (2018) Ghana: Emergency Plan of Action (EPoA) Floods in Upper East Region DREF Operation n° MDRGH015 / PGH031. Available at: https://reliefweb.int/report/ghana/ghana-emergency-plan-action-epoa-floods-upper-east-region-dref-operation-n-mdrgh015. Accessed 24 Nov 2023

IFRC (2019) Ghana: floods in Upper East Region emergency plan of action final report DREF operation n° MDRGH015. "Emergency Plan of Action (EPoA) Ghana / Upper East: Floods". Available at: https://reliefweb.int/report/ghana/ghana-floods-upper-east-region-emergency-plan-action-final-report-dref-operation-n. Accessed 24 Nov 2023

IFRC (2023a) Ghana: floods DREF operational update (MDRGH018). Available at: https://reliefweb.int/report/ghana/ghana-floods-dref-operational-update-mdrgh018-07-november-2023. Accessed 02 Jan 2024

IFRC (2023b) Ghana: imminent floods DREF operation No. MDRGH018. Available at: https://reliefweb.int/report/ghana/ghana-imminent-floods-dref-operation-no-mdrgh018. Accessed 24 Nov 2023

IPCC (2022) Climate change 2022: impacts, adaptation and vulnerability: working group II contribution to the sixth assessment report of the intergovernmental panel on climate change. Cambridge University Press Cambridge. https://doi.org/10.1017/9781009325844

IPCC (2023a) Sections. In: climate change 2023: synthesis report. Contribution of working groups I, II and III to the sixth assessment report of the intergovernmental panel on climate change [Core Writing Team, H. Lee and J. Romero (eds.)]. IPCC, Geneva, Switzerland, 35–115, https://doi.org/10.59327/IPCC/AR6-9789291691647

IPCC (2023b) Summary for policymakers. In: climate change 2023: synthesis report. Contribution of working groups I, II and III to the sixth assessment report of the intergovernmental panel on climate change [Core Writing Team H. Lee and J. Romero (eds.)] IPCC Geneva Switzerland. https://doi.org/10.59327/IPCC/AR6-9789291691647.001

Islam MZ, Wang C (2024) Cost of high-level flooding as a consequence of climate change driver?: A case study of China's flood-prone regions. Ecol Ind 160:111944. https://doi.org/10.1016/j.ecolind.2024.111944

Iqbal M, Rabbani A, Haq F, Bhimani S (2022) The floods of 2022: economic and health crisis hits Pakistan. Ann Med Surg 84. https://doi.org/10.1016/j.amsu.2022.104800

Irvin BC IV, Niemann JD, Perry MA, Bauer KE, McCormick WT III (2023) Parameter estimation for models of major rainfall induced floods in ungaged mountain basins of Colorado. J Hydrol: Reg Stud 45:101300. https://doi.org/10.1016/j.ejrh.2022.101300

Ishola KS, Fatoyinbo AA, Hamid-Mosaku AI, Okolie CJ, Daramola OE, Lawal TO (2023) Groundwater potential mapping in hard rock terrain using remote sensing geospatial and aeromagnetic data. Geosys Geoenviron 2:100107. https://doi.org/10.1016/j.geogeo.2022.100107

Jemai S, Belkendil A, Kallel A, Ayadi I (2024) Assessment of flood risk using hierarchical analysis process method and remote sensing systems through arid catchment in southeastern Tunisia. J Arid Environ 222:105150. https://doi.org/10.1016/j.jaridenv.2024.105150

Jenks G (1967) The data model concept in statistical mapping. Int Yearbook Cartography 7:186–190

Jodhani KH, Patel D, Madhavan N (2021) A review on analysis of flood modelling using different numerical models. Mater Today: Proc. https://doi.org/10.1016/j.matpr.2021.07.405

Juma B, Olang LO, Hassan MA, Chasia S, Mulligan J, Shiundu PM (2023) Flooding in the urban fringes: analysis of flood inundation and hazard levels within the informal settlement of Kibera in Nairobi, Kenya. Phys Chem Earth, Parts A/B/C 132:103499. https://doi.org/10.1016/j.pce.2023.103499

Kaiser M, Günnemann S, Disse M (2021) Spatiotemporal analysis of heavy rain-induced flood occurrences in Germany using a novel event database approach. J Hydrol 595. https://doi.org/10.1016/j.jhydrol.2021.125985

Kannapiran UM, Bhaskar AS (2024) Flood inundation mapping of upstream region in the Adyar River basin: integrating hydrologic engineering centre's river analysis system (HEC-RAS) approach with groundwater considerations. Groundwater for. Sustain Dev 24:101085. https://doi.org/10.1016/j.gsd.2024.101085

Karymbalis E, Andreou M, Batzakis DV, Tsanakas K, Karalis S (2021) Integration of GIS-based multicriteria decision analysis and analytic hierarchy process for flood-hazard assessment in the megalo rema river catchment (East Attica Greece). Sustainability (Switzerland) 13:1–25. https://doi.org/10.3390/su131810232

Kelly AE, Addo H (2023) Ghana's disaster management role and application of information technology. J Emerg Manag Disaster Commun 04:33–62. https://doi.org/10.1142/s2689980923500033

Kordie GA, De-Graft AA, C (2020) Social support in the aftermath of flooding: a study among urban poor dwellers in Accra. Ethiop J Environ Stud Manag 13(3):326–336. https://ejesm.org/doi/v13i3.6. Accessed 20 Aug 2021

Komi K, Amisigo BA, Diekkruger B, Hountondji FCC (2016) Regional flood frequency analysis in the Volta River Basin West Africa. Hydrology 3:1–15. https://doi.org/10.3390/hydrology3010005

Kumar M, Singh P, Singh P (2023) Machine learning and GIS-RS-based algorithms for mapping the groundwater potentiality in the Bundelkhand region India. Ecol Inform 74. https://doi.org/10.1016/j.ecoinf.2023.101980

Kurugama KM, Kazama S, Hiraga Y, Samarasuriya C (2023) A novel hybrid approach of spatial prediction of flood susceptibility in Sri Lanka using bivariate index of entropy and support vector machine models. J JSCE 11:23–7037. https://doi.org/10.2208/journalofjsce.23-27037

Kwang C, Osei Jnr E (2017) Accra flood modelling through application of geographic information systems (GIS) remote sensing techniques and analytical hierarchy process. J Remote Sens GIS 6:191

Leandro J, Shucksmith J (2021) Editorial—modelling of floods in urban areas. Water 13(12):1689. https://doi.org/10.3390/w13121689

Li C, Dash J, Asamoah M, Sheffield J, Dzodzomenyo M, Gebrechorkos SH, Anghileri D, Wright J (2022) Increased flooded area and exposure in the White Volta river basin in Western Africa, identified from multi-source remote sensing data. Sci Rep 12:1–13. https://doi.org/10.1038/s41598-022-07720-4

Liu S, Zhang X, Xu Z, Zhao J, Dong B (2023) Experimental study on the buffering effects of urban trees group in dike-break floods. Sci Rep 13:17096. https://doi.org/10.1038/s41598-023-44024-7

Liuzzo L, Sammartano V, Freni G (2019) Comparison between different distributed methods for flood susceptibility mapping. Water Resour Manage 33(9):3155–3173. https://doi.org/10.1007/s11269-019-02293-w

López-Bermeo C, Montoya RD, Caro-Lopera FJ, Díaz-García JA (2022) Validation of the accuracy of the CHIRPS precipitation dataset at representing climate variability in a tropical mountainous region of South America. Phys Chem Earth 127. https://doi.org/10.1016/j.pce.2022.103184

Miller J, Taylor C, Guichard F, Peyrillé P, Vischel T, Fowe T, Panthou G, Visman E, Bologo M, Traore K, Coulibaly G et al (2022) High-impact weather and urban flooding in the west African Sahel – a multidisciplinary case study of the 2009 event in Ouagadougou. Weather Clim Extrem 36. https://doi.org/10.1016/j.wace.2022.100462

Mishra K, Sinha R (2020) Flood risk assessment in the Kosi megafan using multi-criteria decision analysis: a hydro-geomorphic approach. Geomorphology 350. https://doi.org/10.1016/j.geomorph.2019.106861

Moharir KN, Pande CB, Gautam VK, Singh SK , Rane NL (2023) Integration of hydrogeological data GIS and AHP techniques applied to delineate groundwater potential zones in sandstone limestone and shales rocks of the Damoh district (MP) central India. Environ Res 228. https://doi.org/10.1016/j.envres.2023.115832

Molinari D, De Bruijn KM, Castillo-Rodríguez JT, Aronica GT, Bouwer LM (2019) Validation of flood risk models: current practice and possible improvements. Int J Dis Risk Red 33:441–448. https://doi.org/10.1016/j.ijdrr.2018.10.022

Mwalwimba I, Manda M, Ngongondo C (2024) Measuring vulnerability to assess households resilience to flood risks in Karonga district, Malawi. Nat Hazards. https://doi.org/10.1007/s11069-024-06416-4

Nagamani K, Mishra AK, Meer MS, Das J (2024) Understanding flash flooding in the Himalayan region: a case study. Sci Rep 14(1):7060. https://doi.org/10.1038/s41598-024-53535-w

Nahin KTK, Islam SB, Mahmud S, Hossain I (2023) Flood vulnerability assessment in the Jamuna river floodplain using multi-criteria decision analysis: a case study in Jamalpur district Bangladesh. Heliyon 9. https://doi.org/10.1016/j.heliyon.2023.e14520

Nazeer M, Bork HR (2019) Flood vulnerability assessment through different methodological approaches in the context of North-West Khyber Pakhtunkhwa. Pak Sustain (Switzerland) 11:6695. https://doi.org/10.3390/su11236695

Nazeer M, Bork HR (2021) A local scale flood vulnerability assessment in the flood-prone area of Khyber Pakhtunkhwa, Pakistan. Nat Hazards 105:755–781. https://doi.org/10.1007/s11069-020-04336-7

Ncube S, Wilson A, Petersen L, Black G, Abrams, A, et al. (2023) Understanding resilience capitals agency and habitus in household experiences of water scarcity floods and fire in marginalized settlements in the Cape Flats South Africa. Soc Sci Humanit Open 8. https://doi.org/10.1016/j.ssaho.2023.100710

Nearing G, Cohen D, Dube V, Gauch M, Gilon O, Harrigan S, Hassidim A, Klotz D, Kratzert F, Metzger A, Nevo S, Pappenberger F, Prudhomme C, Shalev G, Shenzis S, Tekalign TY, Weitzner D, Matias Y (2024) Global prediction of extreme floods in ungauged watersheds. Nature 627:559–563. https://doi.org/10.1038/s41586-024-07145-1

Nguyen HD, Fox D, Dang DK, Pham LT, Du QVV, Nguyen THT, Dang TN, Tran VT, Vu PL, Nguyen QH, Nguyen TG, Bui Q, Petrisor A (2021) Predicting future urban flood risk using land change and hydraulic modeling in a river watershed in the central province of Vietnam. Remote Sens 13:1–24. https://doi.org/10.3390/rs13020262

Nsangou D, Kpoumié A, Mfonka Z, Ngouh AN, Fossi DH, Jourdan C, Mbele HZ, Mouncherou OF, Vandervaere JP, Ngoupayou JRN (2022) Urban flood susceptibility modelling using AHP and GIS approach: case of the Mfoundi watershed at Yaoundé in the South-Cameroon plateau. Sci Afr 15:1–16. https://doi.org/10.1016/j.sciaf.2021.e01043

Ntajal J, Lamptey BL, Mahamadou IB, Nyarko BK (2017) Flood disaster risk mapping in the lower Mono River basin in Togo, West Africa. Int J Disaster Risk Reduction 23:93–103. https://doi.org/10.1016/j.ijdrr.2017.03.015

OCHA (2022) West and Central Africa flooding situation - overview, pp 1–3. https://reliefweb.int/report/democratic-republic-congo/west-and-centralafrica-flooding-situation-overview-15-february-2023?gad_source=1&gclid=Cj0KCQjwxeyxBhC7ARIsAC7dS380PdaoJ3KTweFUGgZ1xnDKrpTL8QvFjSBaxmS6sYMBP3NBUo3ubjIaAgClEALw_wcB. Accessed 17 Nov 2023

Ogras S, Onen F (2020) Flood analysis with HEC-RAS: a case study of Tigris River. Adv Civ Eng 1-13. https://doi.org/10.1155/2020/6131982

Okyere CY, Yacouba Y, Gilgenbach D (2013) The problem of annual occurrences of floods in Accra: an integration of hydrological economic and political perspectives. Theoret Empir Res Urban Manag 8:45–79

Osei BK, Ahenkorah I, Ewusi A, Fiadonu EB (2021a) Assessment of flood prone zones in the Tarkwa mining area of Ghana using a GIS-based approach. Environ Challenges 3. https://doi.org/10.1016/j.envc.2021.100028

Osei MA, Amekudzi LK, Omari-Sasu AY, Yamba EI, Quansah E, Aryee JNA, Preko K (2021b) Estimation of the return periods of maxima rainfall and floods at the Pra River Catchment Ghana West Africa using the Gumbel extreme value theory. Heliyon 7:e06980. https://doi.org/10.1016/j.heliyon.2021.e06980

Owusu S, Mul ML, Ghansah B et al (2017) Assessing land suitability for aquifer storage and recharge in northern Ghana using remote sensing and GIS multi-criteria decision analysis technique. Model Earth Syst Environ 3:1383–1393. https://doi.org/10.1007/s40808-017-0360-6

Ozturk D, Safety D (2021) Flood hazard assessment using AHP in corum Turkey flood hazard assessment using AHP in corum Turkey evaluación de peligro de inundación utilizando AHP en corum turquía. Tecnol Ciencias Agua 12:379–415. https://doi.org/10.24850/j-tyca-2021-02-08

Paeth H, Fink AH, Pohle S, Keis F, Mächel H, Samimi C (2011) Meteorological characteristics and potential causes of the 2007 flood in sub-Saharan Africa. Int J Climat 31:1908–1926. https://doi.org/10.1002/joc.2199

Pandey CL, Joseph J, Deshar R, Niraula P (2023) Transboundary flood resilience: insights from Narayani and Mahakali Basins. Int J Dis Risk Red 86. https://doi.org/10.1016/j.ijdrr.2023.103535

Paul GC, Saha S, Hembram TK (2019) Application of the GIS-based probabilistic models for mapping the flood susceptibility in Bansloi Sub-basin of Ganga-Bhagirathi River and their comparison. Remote Sens Earth Syst Sci 2:120–146. https://doi.org/10.1007/s41976-019-00018-6

Pham BT, Luu C, Phong TV, Nguyen HD, Le HV, Tran TQ, Ta HT, Prakash I (2021) Flood risk assessment using hybrid artificial intelligence models integrated with multi-criteria decision analysis in Quang Nam Province Vietnam. J Hydro 592. https://doi.org/10.1016/j.jhydrol.2020.125815

Plataridis K, Mallios Z (2023) Flood susceptibility mapping using hybrid models optimized with Artificial Bee Colony. J Hydro 624. https://doi.org/10.1016/j.jhydrol.2023.129961

Poddar I, Roy R (2024) Application of GIS-based data-driven bivariate statistical models for landslide prediction: a case study of highly affected landslide prone areas of Teesta River basin. Quat Sci Adv 13. https://doi.org/10.1016/j.qsa.2023.100150

Le Polain De Waroux O (2011) Floods as human health risks. Encyclopedia of environmental health, pp 744–755. https://doi.org/10.1016/B978-0-12-409548-9.11462-9

Rączkowska Z, Bucała-Hrabia A, Kędzia S (2024) Triggers of major floods and controls on their geomorphological effects in high-mountain streams (Tatra Mountains, Poland). Catena 239. https://doi.org/10.1016/j.catena.2024.107933

Rahman M, Ningsheng C, Mahmud GI et al (2021) Flooding and its relationship with land cover change population growth and road

density. Geosci Front 12. https://doi.org/10.1016/j.gsf.2021.101224

Rahman ZU, Ullah W, Bai S, Ullah S, Jan MA, Khan M, Tayyab M (2023) GIS-based flood susceptibility mapping using bivariate statistical model in Swat River Basin Eastern Hindukush region Pakistan. Front Environ Sci 11. https://doi.org/10.3389/fenvs.2023.1178540

Ramkar P, Yadav SM (2021) Flood risk index in data - scarce river basins using the AHP and GIS approach. Nat Hazards 109:1119–1140. https://doi.org/10.1007/s11069-021-04871-x

Rana SMS, Habib SMA, Sharifee MNH, Sultana N, Rahman SH (2023) Flood risk mapping of the flood-prone Rangpur division of Bangladesh using remote sensing and multi-criteria analysis. Nat Hazards Res. https://doi.org/10.1016/j.nhres.2023.09.012

Reed C, Anderson W, Kruczkiewicz A, Nakamura J, Gallo D, Seager R, McDermid SS (2022) The impact of flooding on food security across Africa. PANS Environ Sci Sust Sci 119. https://doi.org/10.1073/pnas.2119399119

Rehan ST, Ali E, Sheikh A, Nashwan A (2023) Urban flooding and risk of leptospirosis; Pakistan on the verge of a new disaster: a call for action. Int J Hyg Environ Health 248:114081. https://doi.org/10.1016/j.ijheh.2022.114081

Riazi M, Khosravi K, Shahedi K, Ahmad S, Jun C, Bateni SM, Kazakis N (2023) Enhancing flood susceptibility modeling using multi-temporal SAR images CHIRPS data and hybrid machine learning algorithms. Sci Total Environ 871:162066. https://doi.org/10.1016/j.scitotenv.2023.162066

Roy S, Bose A, Chowdhury IR (2021) Flood risk assessment using geospatial data and multi-criteria decision approach: a study from historically active flood-prone region of Himalayan foothill India. Arab J Geosci 14. https://doi.org/10.1007/s12517-021-07324-8

Saana SBBM, Fosu SA, Sebiawu GE, Jackson N, Karikari T (2016) Assessment of the quality of groundwater for drinking purposes in the Upper West and Northern regions of Ghana. SpringerPlus 5. https://doi.org/10.1186/s40064-016-3676-1

Saaty TL (1977) A scaling method for priorities in hierarchical structures. J Maths Psychol 15:234–281. https://doi.org/10.1016/0022-2496(77)90033-5

Saaty TL (2002) Decision making with the analytical hierarchy process. Scientia Iranica 9:215–229

Saaty TL (2004) Decision making — the analytic hierarchy and network processes (AHP/ANP). J Syst Sci Syst Eng 13. https://doi.org/10.1007/s11518-006-0151-5

Sachdeva S, Kumar B (2022) Flood susceptibility mapping using extremely randomized trees for Assam 2020 floods. Ecol Inform 67. https://doi.org/10.1016/j.ecoinf.2021.101498

Sacré Regis MD, Mouhamed L, Kouakou K, Adeline B, Arona D, Houebagnon Saint JC, Koffi Claude AK, Talnan Jean HC, Salomon O, Issiaka S (2020) Using the CHIRPS dataset to investigate historical changes in precipitation extremes in West Africa. Clim 8. https://doi.org/10.3390/CLI8070084

Saksena S, Dey S, Merwade V, Singhofen PJ (2020) A computationally efficient and physically based approach for urban flood modeling using a flexible spatiotemporal structure. Wat Res 56.https://doi.org/10.1029/2019WR025769

Samela C, Persiano S, Bagli S, Luzzi V, Mazzoli P, Humer G, Reithofer A, Essenfelder A, Amadio M, Mysiak J, Castellarin A (2020) Safer_RAIN: a DEM-based hierarchical filling-&-spilling algorithm for pluvial flood hazard assessment and mapping across large urban areas. Water 12:1514. https://doi.org/10.3390/w12061514

Santosa BH, Martono DN, Purwana R, Koestoer R (2022) Flood vulnerability evaluation and prediction using multi-temporal data: a case in Tangerang, Indonesia. Int J Adv Sci Eng Inform Technol 12:2156–2164. https://doi.org/10.18517/ijaseit.12.6.16903

Sayers W et al (2014) Artificial intelligence techniques for flood risk management in urban environments. Procedia Eng 70:1505–1512. https://doi.org/10.1016/j.proeng.2014.02.165

Schober P, Schwarte LA (2018) Correlation coefficients: appropriate use and interpretation. Anesth Analg 126:763–1768. https://doi.org/10.1213/ANE.0000000000002864

Seemuangngam A, Lin H (2024) The impact of urbanization on urban flood risk of Nakhon Ratchasima Thailand. Appl Geogr 162. https://doi.org/10.1016/j.apgeog.2023.103152

Shaikh AA, Pathan AI, Waikhom SI, Agnihotri PG, Islam MN, Singh SK (2023) Application of latest HEC-RAS version 6 for 2D hydrodynamic modeling through GIS framework: a case study from coastal urban floodplain in India. Model Earth Syst Environ 9:1369–1385. https://doi.org/10.1007/s40808-022-01567-4

Shekar PR, Mathew A (2023a) Assessing groundwater potential zones and artificial recharge sites in the monsoon-fed Murredu river basin India: an integrated approach using GIS AHP and Fuzzy-AHP. Groundwater Sust Develop 23.https://doi.org/10.1016/j.gsd.2023.100994

Shekar PR, Mathew A (2023b) Flood susceptibility mapping of the Peddavagu River Basin using GIS-AHP techniques. Develop Environ Sci. 1st ed. Elsevier B.V. https://doi.org/10.1016/B978-0-443-18640-0.00011-0

Singer, M (2018) Climate Change and Social Inequality: The Health and Social Costs of Global Warming (1st ed.). Routledge. https://doi.org/10.4324/9781315103358

Slimani FE, Zghibi A, Elomri A, Aloui S, Naeem K, Merzougui A, Msaddek MH, Chekirbene A (2023) Identification of groundwater potential recharge zones in a Tunisian anthropogenic coastal region: insights from multi-criteria decision-making techniques. J Afr Earth Sci 209:105108. https://doi.org/10.1016/j.jafrearsci.2023.105108

Smits WK, Attoh EMNAN, Ludwig F (2024) Flood risk assessment and adaptation under changing climate for the agricultural system in the Ghanaian White. Clim Change 177.https://doi.org/10.1007/s10584-024-03694-6

Sofia G, Nikolopoulos EI (2020) Floods and rivers: a circular causality perspective. Sci Rep 10:1–17. https://doi.org/10.1038/s41598-020-61533-x

Soussa H, El Feel AA, Alfy SZ, Yousif MS (2012) Flood hazard in Wadi Rahbaa area Egypt. Arab J Geosciences 5:45–52. https://doi.org/10.1007/s12517-010-0144-z

Srivastava S, Roy T (2023) Integrated flood risk assessment of properties and associated population at county scale for Nebraska, USA. Sci Rep 13:19702. https://doi.org/10.1038/s41598-023-45827-4

Suwanno P, Yaibok C, Pornbunyanon T, Kanjanakul C, Buathongkhue C, Tsumita N, Fukuda A (2023) GIS-based identification and analysis of suitable evacuation areas and routes in flood-prone zones of Nakhon Si Thammarat municipality. IATSS Res 47:416–431. https://doi.org/10.1016/j.iatssr.2023.08.004

Swain KC, Singha C, Nayak L (2020a) Flood susceptibility mapping through the GIS-AHP technique using the cloud. ISPRS Int J Geo-Inform 9. https://doi.org/10.3390/ijgi9120720

Swain KC, Singha C, Nayak L (2020b) Flood susceptibility mapping through the GIS-AHP technique using the cloud. ISPRS Int J Geo-Inform 9:720. https://doi.org/10.3390/ijgi9120720

Tabari H (2020) Climate change impact on flood and extreme precipitation increases with water availability. Sci Rep 10:13768. https://doi.org/10.1038/s41598-020-70816-2

Tamiru H, Wagari M (2022) Machine-learning and HEC-RAS integrated models for flood inundation mapping in Baro River Basin, Ethiopia. Model Earth Syst Environ 8:2291–2303. https://doi.org/10.1007/s40808-021-01175-8

Taraky YM, Liu Y, Mcbean E, Daggupati P, Gharabaghi B (2021) Flood risk management with transboundary conflict and

cooperation dynamics in the Kabul River Basin. Water 13:1513. https://doi.org/10.3390/w13111513

Tarasova L, Lun D, Merz R, Blöschl G, Basso S, Bertola M, Miniussi A, Rakovec O, Samaniego L, Thober S, Kumar R (2023) Shifts in flood generation processes exacerbate regional flood anomalies in Europe. Commun Earth Environ 4:49. https://doi.org/10.1038/s43247-023-00714-8

Tariq A, Beni LH, Ali S, Adnan S, Hatamleh WA (2023) An effective geospatial-based flash flood susceptibility assessment with hydrogeomorphic responses on groundwater recharge. Groundwater Sust Develop 23:100998. https://doi.org/10.1016/j.gsd.2023.100998

Tegegne AM, Lohani T K, Eshete AA (2024) Groundwater potential delineation using geodetector based convolutional neural network in the Gunabay watershed of Ethiopia. Environ Res 242. https://doi.org/10.1016/j.envres.2023.117790

Tesselaar M, Botzen WJW, Tiggeloven T, Aerts JCJH (2023) Flood insurance is a driver of population growth in European floodplains. Nat Commun 14:7483. https://doi.org/10.1038/s41467-023-43229-8

The World Bank Group.(2021) "Climate Risk country profile: Ghana"

Toosi AS, Calbimonte GH, Nouri H, Alaghmand S (2019) River basin-scale flood hazard assessment using a modified multi-criteria decision analysis approach: a case study. J Hydro 574:660–671. https://doi.org/10.1016/j.jhydrol.2019.04.072

Tramblay Y, Villarini G, Saidi ME, Massari C, Stein L (2022) Classification of flood - generating processes in Africa. Sci Rep 12:18920. https://doi.org/10.1038/s41598-022-23725-5

Tripathi R, Sengupta SK, Patra A, Chang H, Jung IW (2014) Climate change urban development and community perception of an extreme flood: a case study of Vernonia Oregon USA. Appl Geography 46:137–146. https://doi.org/10.1016/j.apgeog.2013.11.007

Twum KO, Abubakari M (2019) Cities and floods: a pragmatic insight into the determinants of households' coping strategies to floods in informal Accra, Ghana. Jàmbá: J Disaster Risk Stud 11:a608. https://doi.org/10.4102/jamba.v11i1.608

Ullah K, Zhang J (2020) GIS-based flood hazard mapping using relative frequency ratio method: a case study of Panjkora River Basin, eastern Hindu Kush, Pakistan. Plos One 15(3):e0229153. https://doi.org/10.1371/journal.pone.0229153

Upadhyay S, Silwal P, Prajapati R, Talchabhadel R, Shrestha S, Duwal S, Lakhe H (2022) Evaluating magnitude agreement and occurrence consistency of CHIRPS product with ground-based observations over medium-sized river basins in Nepal. Hydrology 9. https://doi.org/10.3390/hydrology9080146

UNESCO (2023a) "Best practices on flood and drought risk management. Edited by R. Marteleira. Paris France: United Nations Educational Scientific and Cultural Organization". Available at: https://unesdoc.unesco.org/ark:/48223/pf0000384487. Accessed 18 Dec 2023

UNESCO (2023b) Learning at risk: the impact of climate displacement; Global Report. France: United Nations Educational Scientific and Cultural Organization. Available at: https://unesdoc.unesco.org/ark:/48223/pf0000387895. Accessed 18 Dec 2023

UNISDR (2015) The human cost of natural disasters: a global perspective. Available at: https://reliefweb.int/report/world/human-cost-natural-disasters-2015-global-perspective. Accessed 10 Feb 2023

United Nations (2007) Office of the Resident Coordinator of the United Nations. In: Ghana: Situation report on floods, vol 3, pp 1–8. https://reliefweb.int/report/ghana/ghana-situation-report-floods-11-oct-01-nov-2007. Accessed 6 Apr 2023

United Nations (2009) "The United Nations world water development report 3: water in a changing world". Paris: UNESCO and London: Earthscan. Available at: https://digitallibrary.un.org/record/3895839?ln=en&v=pdf. Accessed 28 Jan 2022

Wang Y, Hong H, Chen W, Li S, Panahi M, Khosravi K, Shirzadi A, Shahabi H, Panahi S, Costache R (2019) Flood susceptibility mapping in Dingnan County (China) using adaptive neuro-fuzzy inference system with biogeography based optimization and imperialistic competitive algorithm. J Environ Manag 247:712–729. https://doi.org/10.1016/j.jenvman.2019.06.102

Wani MJ, Sarda VK, Jain SK (2017) Assessment of trends and variability of rainfall and temperature for the district of Mandi in Himachal Pradesh India. Slovak J Civil Eng 25:15–22. https://doi.org/10.1515/sjce-2017-0014

Wicaksono AD, Hidayah E, Wiyono RUA (2021) Flood vulnerability assessment of kali welang floodplain by using analytic hierarchy process based methods. UKaRsT 5. https://doi.org/10.1016/j.gloenvcha.2006.03.008

WMO (2022) State of the global climate 2021. World Meteorological Association, Switzerland. https://library.wmo.int/viewer/66214/download?file=Statement_2022.pdf&type=pdf&navigator=1. Accessed 8 May 2024

World Economic Forum (2024) "The Global risks report 2024. 9th Edition. Insight report.World economic forum". Available at: https://www.weforum.org/publications/global-risks-report-2024/. Accessed 13 Jan 2023

Wubalem A, Tesfaw G, Dawit Z et al (2021) Comparison of statistical and analytical hierarchy process methods on flood susceptibility mapping: In a case study of the Lake Tana sub-basin in northwestern Ethiopia. Open Geosci 13:1668–1688. https://doi.org/10.1515/geo-2020-0329

Yang F, Xiong S, Ou J, Zhao Z, Lei T (2022) Human settlement resilience zoning and optimizing strategies for river-network cities under flood risk management objectives: Taking Yueyang City as an example. Sustainability (Switzerland) 14. https://doi.org/10.3390/su14159595

Yin Q, Ntim-Amo G, Ran R, Xu D, Ansah S, Hu J, Tang H (2021) Flood disaster risk perception and urban households' flood disaster preparedness: the case of Accra metropolis in Ghana. Water (Switzerland) 13. https://doi.org/10.3390/w13172328

Yin Q, Ntim-Amo G, Xu D, Gamboc VK, Ran R, Hu J, Tang H (2022) Flood disaster risk perception and evacuation willingness of urban households: the case of Accra, Ghana. Int J Disaster Risk Reduct 78:103126. https://doi.org/10.1016/j.ijdrr.2022.103126

Yu H, Luo Z, Wang L, Ding X, Wang S (2023a) Improving the accuracy of flood susceptibility prediction by combining machine learning models and the expanded flood inventory data. Remote Sens 15:3601. https://doi.org/10.3390/rs15143601

Yu H, Luo Z, Wang L, Ding X, Wang S (2023b) Improving the accuracy of flood susceptibility prediction by combining machine learning models and the expanded flood inventory data. Remote Sens 5:3601. https://doi.org/10.3390/rs15143601

Ziwei L, Xiangling T, Liju L, Yanqi C, Xingming W, Dishan Y (2023) GIS-based risk assessment of flood disaster in the Lijiang River Basin. Sci Rep 13:6160. https://doi.org/10.1038/s41598-023-32829-5

Authors and Affiliations

Benjamin Wullobayi Dekongmen[1,2] ⓘ **· Amos Tiereyangn Kabo-bah[1] · Geophrey Kwame Anornu[3] · Komlavi Akpoti[4] · Mark Amo-Boateng[5] · Eric Ofosu Antwi[1,6] · Edward Oppong Boamah[7] · Emmanuel Daanoba Sunkari[8,9]**

✉ Benjamin Wullobayi Dekongmen
  dekongmen@gmail.com

[1] Department of Civil and Environmental Engineering, University of Energy and Natural Resources (UENR), P.O. Box 214, Sunyani, Ghana

[2] Department of Agricultural Engineering, Ho Technical University, Post Office Box HP217, Ho, Ghana

[3] Department of Civil Engineering, Regional Water and Environmental Sanitation Centre Kumasi (RWESCK), Kwame Nkrumah University of Science and Technology, Kumasi, Ghana

[4] International Water Management Institute (IWMI), Accra, Ghana

[5] Department of Civil and Environmental Engineering, University of Missouri, Columbia, MO, USA

[6] Regional Centre for Energy and Environmental Sustainability (RCEES), University of Energy and Natural Resources (UENR), P.O. Box 214, Sunyani, Ghana

[7] Digital Earth Africa, Pretoria, South Africa

[8] Department of Geological Engineering, Faculty of Geosciences and Environmental Studies, University of Mines and Technology, P.O. Box 237, Tarkwa, Ghana

[9] Department of Chemical Sciences, Faculty of Science, University of Johannesburg, Auckland Park 2006, Kingsway Campus, P.O. Box 524, Johannesburg, South Africa